symmetry

MDPI

Article

Explicit Closed-Form Expression for Run-Length Evaluation of the Double-Modified EWMA Control Chart Under ARX and ARFIX Models: Application to Major Crude Oil Benchmarks

Kotchaporn Karoon [1], Saowanit Sukparungsee [2] and Yupaporn Areepong [2,*]

[1] Department of Mathematics, Faculty of Science, Naresuan University, Phitsanulok 65000, Thailand; kotchapornk@nu.ac.th
[2] Department of Applied Statistics, Faculty of Applied Science, King Mongkut's University of Technology North Bangkok, Bangkok 10800, Thailand; saowanit.s@sci.kmutnb.ac.th
* Correspondence: yupaporn.a@sci.kmutnb.ac.th

Abstract

Control charts are used in statistical process control (SPC) to keep track of processes and identify changes in the way that they work. The control limits around the center line are uniform, which means they react the same way to changes going in either direction. In contrast, linear charts use imbalance to make it easier to identify individual data points. Therefore, using imbalance in the creation of control charts helps keep track of and maintain consistency with data that has a big impact on results when it goes beyond predetermined limits. In this study, we look at both one-sided and two-sided control charts by getting an explicit closed-form formula for the double-modified EWMA control chart's average run length (ARL). The study is mostly about developing better ways to spot things using autoregressive fractionally integrated models and external variables (ARX and ARFIX) in the presence of exponential white noise. The ARL is used to test how well the proposed chart works in both modeling systems. The NIE method is used to prove that the explicit closed-form ARL formula works. The closed-form ARL expression is shown to be valid under the given ARX and ARFIX model assumptions, exponential white noise errors, stationarity conditions, and fixed one-sided or two-sided control limits. The results show that %RPC has a value below 10^{-6}, and the computation times for the ARX and ARFIX models remain below 1.6 s and 3 s, respectively, after that point. To show how much better it is, the suggestion is compared to Type-EWMA control charts, such as classical and modified EWMA charts, in terms of run-length efficiency using ARL and SDRL, as well as overall efficiency by the relative index and with mean and standard deviation. The simulation study checks how well the proposed chart works in both symmetric two-sided and asymmetric one-sided frameworks. For the crude oil application, the one-sided upper control chart is used to detect abrupt upward price shifts, which may indicate precautionary demand shocks, market uncertainty, and risk spillovers to financial markets. According to the findings, the suggested chart is able to identify shifts at a faster rate than both traditional EWMA charts and modified EWMA charts, which demonstrates that it is beneficial in a real setting.

Keywords: statistical process control; double-modified EWMA; control chart; average run length; numerical integral equation

Check for updates

Received: 10 May 2026
Revised: 1 June 2026
Accepted: 8 June 2026
Published: 11 June 2026

Copyright: © 2026 by the authors. Licensee MDPI, Basel, Switzerland. This article is an open access article distributed under the terms and conditions of the Creative Commons Attribution (CC BY) license.

1. Introduction

Statistical process control is a way of observing events as they occur. The good news is it can detect abnormal activity and tell you how solid things are. SPC employs control charts to detect faults and trends for quick response. It is widely used in industry, finance, environmental monitoring, healthcare as shown in [1–3], etc. Control charts are very useful as in real-life applications as in statistical process control (SPC). For instance, Alshahrani et al. [4] proposed a Bayesian Shewhart chart to monitor the drilling process. The advantages of an improved EWMA chart in industry have been discussed by Anwar et al. [5] especially for process control in the wood industry. Time-series data often have persistent structural shifts, autocorrelation, and long-memory effects. Such features may lead to a loss of effectiveness of the standard control charts and to biased or inconsistent detection in dynamic environments. This problem is especially relevant in finance and economics, where the correct detection of both upward and downward movements is essential to monitor volatility, evaluate risk, and detect abnormal market behavior. Symmetry is an important aspect in such contexts, as positive and negative changes may contain equally meaningful information. A symmetric view encourages neutrality, aids an even-handed interpretation, and minimizes the directional bias in statistical evaluation. Economic and financial series are often subject to volatility, uncertainty, and structural change, and symmetry provides a useful basis for the use of control charts to monitor and detect shifts. The crude oil benchmark series, especially WTI and Brent, are an important empirical setting for this study, as they are the two main crude oil reference prices in the global oil trading and are international benchmarks for price discovery and the determination of crude oil prices worldwide [6,7].

Control charts are basic tools in SPC for monitoring process behavior and identifying shifts over time. In dynamic situations it is important that the device is equally sensitive to upward and downward movement and this is achieved by symmetry. The Shewhart control chart, proposed by Shewhart [8], is one of the most popular tools for process monitoring and is especially good at detecting large shifts. However, for small-to-moderate shifts, more sensitive charts like CUSUM and EWMA are often preferred. Page [9] and Roberts [10] are the originators of these charts respectively. The EWMA control chart was then extended to other areas. Several Type-EWMA control charts have been developed to enhance sensitivity and improve monitoring efficiency, especially for detecting small shifts in different process conditions. Modified Exponentially Weighted Moving Average (modified EWMA) control chart introduced by Patel and Divecha [11] and later verified and elaborated by Khan et al. [12]; Double Exponentially Weighted Moving Average (double EWMA) control chart proposed by Shamma and Shamma [13]; Extended Exponentially Weighted Moving Average (extended EWMA) control chart proposed by Naveed et al. [14]. Supplementary control charts were then constructed based on Type-EWMA structures including the extended EWMA and modified EWMA charts. These further studies include the new extended EWMA control chart proposed by Javed et al. [15] and the double-modified EWMA control chart proposed by Alevizakos et al. [16]. The charts were developed to improve detection sensitivity and the overall effectiveness of monitoring, especially for small changes. The main focus of this research is to develop the performance of the double-modified EWMA control chart.

Control chart performance is considered under time-series models with exogenous variables to help solve serial dependency. Autoregressive models with exogenous variables (ARX and ARFIX) are particularly useful since they can represent external inputs, persistence, and long-range dependence in economic and financial series. The importance of these properties is due to the fact that unmodeled autocorrelation can affect control chart performance and reliability significantly. ARX allows capturing short-memory dependence

with exogenous effects, and ARFIX allows capturing long-memory dependence more readily through fractional integration. Real-data applications are encouraged for their practical value. ARX-type models are used for Brazilian securities [17], day-ahead electricity price forecasting with exogenous demand and wind-power variables [18], and electricity consumption forecasting with external climatic and pandemic factors [19]. Therefore, ARX and ARFIX are of particular interest in the present study because of their flexibility and applicability to data from many fields to evaluate control chart performance in dynamic real-world settings.

In this context, the main measure for evaluating the performance of a control chart is the average run length (ARL): the number of samples one expects to be taken before the control chart signals a problem. The ARL has two states: the in-control state, ARL_0, which we want to be large to reduce false alarms, and the out-of-control state, ARL_1, which we want to be small so that we can detect process changes quickly. In practice, when something changes in the process, the control chart should quickly inform us if corrective action or more inquiry is needed. The ARL can be computed in different ways in the literature, such as the Markov chain approach, Monte Carlo simulation and numerical integral equation (NIE) approaches [20–22].

Among the existing strategies, explicit closed-form formulas are of particular interest, as they allow for fast and efficient evaluation of ARL, usually at a lower computational cost than numerical or simulation-based methods. This approach can be combined with time-series models such as ARMA and ARFIMA models to develop an effective analysis of real-world data today. The accuracy of ARL for the modified EWMA control chart was superior to the NIE technique and required less time to compute. The technique was built under the ARFI concept seen in [23] and was verified using a monthly dataset of pneumonia incidence in Thailand and a daily dataset of Netflix stock prices.

They then showed that it could be used by using real monthly and quarterly data on durian exports. Polyeam and Phanyaem [24] proposed an explicit closed-form ARL for the EWMA control chart under a seasonal autoregressive process with a quadratic trend and applied it to monthly lobar pneumonia data from Siriraj Hospital in Bangkok, Thailand, covering January 2019 to December 2024. Similarly, Jirawattanapalin and Phanyaem [25] in 2026 built an explicit closed-form ARL for the EWMA chart under an autoregressive process with quadratic trend and showed the procedure for pneumonia data in the same hospital. Karoon and Areepong [26] also presented an explicit closed-form ARL for the new modified EWMA control chart under ARI and ARFI time-series models and ran U.S. stock price data to illustrate its capacity. The classical ARMA and ARFIMA model has been generalized through the inclusion of exogenous variables, giving rise to the ARFIMAX model framework. The benefits of this model are improved accuracy and robustness of forecasting through explicitly incorporating the external drivers, thus providing better flexibility and realistic representation of the complex economic systems. At the beginning, Paichit et al. [27] derive exact equations for the ARL of the EWMA chart for an ARX(p) process with exponential white noise and show great agreement and high accuracy when compared to the numerical integral equation solutions based on the Gauss–Legendre method.

The long-memory characteristic often seen in time-series data is the reason for the usage of the ARFIX model. The control chart in the suggested ARFIX framework with the fractional integration may accommodate the lengthy memory reliance of the ARL performance. Moreover, Okhrin and Schmid (2019) [28] studied the run-length behavior of EWMA charts under long-memory dependency for long-memory processes and showed that the dependence structure of the underlying process is important for the performance of charts. This study shows that the fractional integration is needed in the evaluation of the

ARL performance of control charts of time series. Hence, ARL is a reasonable criterion to evaluate and compare the effectiveness of control charts for ARX and ARFIX models.

Next, Silpakob et al. [29] determined the ARL of the modified EWMA chart for an ARX(p) process. In the modified EWMA control chart, the explanatory variable was the price of diesel oil, which was illustrated by the real data of cassava prices. In 2022, Bualuang and Peerajit [30] derived an accurate ARL for the CUSUM control chart. The accuracy and computing speed of the new ARL are better than those of the NIE technique. They use the USD/THB exchange rate and real data from the K-CHANGE-A (A) fund and the gold futures pricing to show the system in action. Recently, Peerajit [31] proposed an exact ARL for the EWMA control chart, with better computing efficiency and accuracy than the NIE technique. The framework is built on the LSFIMAX model with exponential white noise and assessed using ARL-based metrics. The model was validated using economic data, with the main focus on monthly power output, treating natural gas and electricity exports as one and two exogenous variables respectively.

On the double-modified EWMA control chart, the ARL under dependent processes, such as ARX and ARFIX models, is not well-defined in the existing literature, especially when dealing with exponential white noise, even though control charts have been the subject of much study. As a result, we provide the ARL of the double-modified EWMA control chart for general AR with exogenous and fractionally integrated exogenous time-series models, as well as general ARX and ARFIX models. We used both the NIE method and the explicit closed-form ARL solution to finish the calculation. The accuracy and calculation speed of the two methods were compared using the one- and two-sided double-modified EWMA control charts. The suggested double-modified EWMA chart based on both simulated and real-world major crude oil benchmarks with two exogenous variables (US Dollar Index and Volatility Index) and two exogenous variables (WTI crude oil prices and US treasury 10Y yield) for WTI and Brent, respectively, was then compared to the traditional EWMA and modified EWMA control charts.

This study extends previous work on modified EWMA control charts for ARX processes [29] and presents several important extensions. First, the proposed chart is designed as a double-modified EWMA control chart under ARX and ARFIX models. Specifically, the ARFIX model uses fractional integration to model long-memory dependence in time-series processes. To the best of our knowledge, the application of ARX and ARFIX models to the double-modified EWMA control chart has not been fully studied in previous research. Furthermore, explicit closed-form ARL expressions are derived for both the one-sided and two-sided control limits, and they are validated using the numerical integral equation method. The proposed chart is further applied to major crude oil benchmarks and compared with several EWMA-type control charts. These extensions differentiate the current study from the other ARX-based modified EWMA studies.

2. Preliminaries

2.1. The Autoregressive with Exogenous Variables; ARX Model

An autoregressive model with external variables (ARX model) is used to characterize the present values of the response variable as a function of the past values and external explanatory factors. Its simple structure and interpretability make it useful for modeling systems influenced by both internal dynamics and external factors. Equation (1) presents the operator form of the ARX(p, r) model.

$$y_t = \vartheta + \sum_{i=1}^{p} \phi_i y_{t-i} + \sum_{j=1}^{r} b_j x_{t-j} + \varepsilon_t, \tag{1}$$

where y_t is the response variable, y_{t-i} are its lagged values, x_{t-j} are the exogenous variables, b_j are their corresponding coefficients, p represents the autoregressive order, r signifies the number of delayed exogenous variables, and ε_t specifies an exponential white noise error term.

2.2. The Autoregressive Fractionally Integrated Model with Exogenous Variables; ARFIX Model

The autoregressive fractionally integrated model with exogenous variables (ARFIX) extends the ARFI model by incorporating exogenous variables, allowing the model to capture both long-memory dependence and external effects. To illustrate the dynamic structure of the process, Equation (2) combines the autoregressive polynomial, the differencing operator, and exogenous variables to present the operator form of the ARFIX(p, d, r) model. The ARFIX(p, d, r) model can generally be written as

$$\phi(B)(1-B)^d y_t = \vartheta + \sum_{j=1}^{r} b_j x_{t-j} + \varepsilon_t, \quad 0 < d < 1, \tag{2}$$

where $\phi(B) = 1 - \phi_1 B - \phi_2 B^2 - \cdots - \phi_p B^p$.

Consequently, by augmenting the backshift operator, the model may be articulated as

$$(1-B)^d y_t = \vartheta + \phi_1 y_{t-1} + \phi_2 y_{t-2} + \cdots + \phi_p y_{t-p} + b_1 x_{t-1} + b_2 x_{t-2} + \cdots + b_r X_{t-r} + \varepsilon_t.$$

Under this condition, $(1-B)^d$ admits the following infinite binomial expansion in (3)

$$(1-B)^d = \sum_{k=0}^{\infty} \binom{d}{k} (-B)^k = 1 - dB + \frac{d(d-1)}{2!} B^2 - \frac{d(d-1)(d-2)}{3!} B^3 + \cdots \tag{3}$$

where B denotes the backward-shift operator, k is the summation index, and d denotes the fractional differencing order, where $0 < d < 0.5$ ensures process stability [32]. This expansion represents the fractional differencing operator in infinite binomial series form. Moreover, the ARFIX process is based on long memory through fractional integration. This is in contrast to the ARX model, where only a few lag terms are used to set up the dependency structure. In contrast, the ARFIX model allows past observations to continuously influence the current level of the process. That means the estimate takes longer because it needs to consider more past relationships. This makes the ARX model different from ARFIX.

Furthermore, the fractional integration is added to capture the long-memory behavior, which is often found in time-series data. It was shown in previous studies that for long-memory processes the dependence structure may affect the run-length distribution and ARL performance of EWMA charts [28]. So the proposed chart can model the persistent dependence and assess the run-length behavior by considering the ARFIX model.

2.3. The Structures of the Modified EWMA Control Chart

At the start, the modified EWMA chart was first introduced by Patel and Divecha [11] and later refined by Khan et al. [12] to improve the detection of small-to-moderate process shifts. Its charting statistic is defined in Equation (4).

$$\Xi_t = (1-\lambda)\Xi_{t-1} + \lambda y_t + \kappa(y_t - y_{t-1}), \quad t = 1, 2, 3, \ldots, \tag{4}$$

where $\kappa > 0$ is a constant, Ξ_{t-1} denotes the previous modified EWMA value, and $\Xi_0 = u$ is the initial value. The case $\kappa = 1$ corresponds to the modified EWMA chart [11]. The mean and variance of Ξ_t are $E(\Xi_t) = \mu$ and $\mathrm{Var}(\Xi_t) = \frac{(\lambda + 2\lambda\kappa + 2\kappa^2)\sigma^2}{2-\lambda}$, respectively.

The process is monitored by the control limits given in (5), representing the upper control limit (UCL) and lower control limit (LCL):

$$\text{UCL/LCL} = \mu \pm £_1\sigma\sqrt{\frac{\lambda + 2\lambda\kappa + 2\kappa^2}{2-\lambda}}. \tag{5}$$

Accordingly, the stopping time of the modified EWMA control chart can be defined as

$$\tau_{H_1} = \inf\{t \geq 0 : \Xi_t < \text{LCL or } \Xi_t > \text{UCL}\}.$$

When $\kappa = 0$, the modified EWMA chart reduces to the classical EWMA chart with control limits

$$\text{UCL/LCL} = \mu \pm £_0\sigma\sqrt{\frac{\lambda}{2-\lambda}}.$$

2.4. The Structures of the Double-Modified EWMA Control Chart

By adding an extra smoothing step to the modified EWMA chart, the double-modified EWMA control chart was created. This change enhances the overall performance of the charts and makes monitoring more sensitive. Alevizakos et al. [16] were the first to suggest it.

$$\begin{aligned} \Xi_t &= (1-\lambda_1)\Xi_{t-1} + \lambda_1 y_t + \kappa_1(y_t - y_{t-1}), \\ \Psi_t &= (1-\lambda_2)\Psi_{t-1} + \lambda_2\Xi_t + \kappa_2(\Xi_t - \Xi_{t-1}), \end{aligned} \tag{6}$$

where y_t is the observation at time t, Ξ_t denotes the modified EWMA statistic, and Ψ_t denotes the double-modified EWMA statistic. The parameters λ_1 and λ_2 are smoothing constants satisfying $0 < \lambda_1, \lambda_2 \leq 1$, whereas κ_1 and κ_2 are modification coefficients. In general, moderate parameter values are recommended to balance detection sensitivity and robustness. In this study, λ is assigned to λ_2, with $\lambda_2 \in [0.05, 0.10, 0.15]$, $\lambda_1 = 2\lambda_2$, and $\kappa_1, \kappa_2 \in \{1, 3, 9\}$. For the special case $\lambda_1 = \lambda_2 = \lambda$ and $\kappa_1 = \kappa_2 = \kappa$, the mean of the double-modified EWMA statistic is $E(\Psi) = \mu$. While, $\theta = (1-\lambda)^2$, $\nu = (\kappa+\lambda)^2$ and $\varsigma = (\kappa+\lambda-1)^2$, the variance in the statistic of Ψ_t is given by

$$\frac{\text{Var}(\Psi_t)}{\sigma^2} = \nu^2 + 4\lambda^2\nu\varsigma + \frac{4\lambda^2\nu\varsigma\theta}{1-\theta} - \frac{4\lambda^3\varsigma(\kappa+\lambda)(\kappa+\lambda-1)(1-\lambda)}{(1-\theta)^2} + \lambda^4\varsigma^2\frac{1+\theta}{(1-\theta)^3}.$$

Accordingly, the center line and control limits of the double-modified EWMA chart are shown in (7) as

$$\text{UCL/LCL} = \mu \pm £\sigma\sqrt{\text{Var}(\Psi_t)}. \tag{7}$$

where $£ > 0$ is the control limit coefficient, and σ denotes the process standard deviation. Moreover, the stopping time of this is

$$\tau_H = \inf\{t \geq 0 : \Psi_t < \text{LCL or } \Psi_t > \text{UCL}\}.$$

3. Derivation of Run-Length Evaluation on the Double-Modified EWMA Control Chart with Exponential White Noise

3.1. ARL Derivation Under an AR Model with Exogenous Variables

Under the ARX(p, r) framework, the autoregressive process is extended by incorporating exogenous variables to capture the influence of external factors on the process behavior. This study derives the explicit closed-form ARL expression and compares its performance with the numerical integral equation (NIE) method for the ARX(p, r) model. The derived closed-form ARL expression is applicable under fixed proposed model parameters,

exponential white noise innovations, and the stationarity requirement of the underlying time-series process and makes use of both one-sided or two-sided control limits.

3.1.1. Steps of Deriving the Explicit Closed-Form ARL Solution Under ARX(p, r) Model

Step 1: Substitution and control interval. Substituting y_t from Equation (1) into the double-modified EWMA statistic Ψ_t in Equation (6), and setting $t = 1$ with $\Psi_0 = v$, $\Xi_0 = u$, and $\eta = (\lambda_1\lambda_2 + \kappa_1\lambda_2 + \kappa_2\lambda_1 + \kappa_1\kappa_2)$, Ψ_1 shown as

$$(1-\lambda_2)v - (\lambda_1\lambda_2 + \lambda_1\kappa_2 - \lambda_2)u + \eta(\vartheta + \sum_{i=1}^{p}\phi_i y_{1-i} + \sum_{j=1}^{r} b_j x_{1-j} + \varepsilon_1) - (\kappa_1\lambda_2 + \kappa_1\kappa_2)\omega.$$

Under controlled conditions, the relevant control period can be expressed as $l < \Psi_1 < h$, and this can be further explained by the equation below.

$$l < (1-\lambda_2)v - (\lambda_1\lambda_2 + \lambda_1\kappa_2 - \lambda_2)u - (\kappa_1\lambda_2 + \kappa_1\kappa_2)\omega + \eta\vartheta + \eta\sum_{j=1}^{r} b_j x_{1-j} + \eta\varepsilon_1 < h.$$

Step 2: Rearrangement in terms of $L < \varepsilon_1 < H$.
Rearranging the equations from Step 1 above to form interval ε_1, as follows:

$$\frac{l - \rho v + Qu + Q'\omega}{\eta} - \vartheta - \sum_{j=1}^{r} b_j x_{1-j} < \varepsilon_1 < \frac{h - \rho v + Qu + Q'\omega}{\eta} - \vartheta - \sum_{j=1}^{r} b_j x_{1-j}$$

Let L and H represent $\frac{l-\rho v+Qu+Q'\omega}{\eta} - \vartheta - \sum_{j=1}^{r} b_j x_{1-j}$, and $\frac{h-\rho v+Qu+Q'\omega}{\eta} - \vartheta - \sum_{j=1}^{r} b_j x_{1-j}$, respectively. Thus, the interval of ε_1, it can be shown as $L < \varepsilon_1 < H$, and then, $Q = (\lambda_1\lambda_2 + \lambda_1\kappa_2 - \lambda_2)$, $Q' = (\kappa_1\lambda_2 + \kappa_1\kappa_2)$, and $1 - \lambda_2$ represents ρ .

Step 3: Fredholm integral equation. Let $\Pi(v)$ be the ARL function of the double-modified EWMA chart under the ARX(p, r) model. Following the Fredholm integral equation approach [33], and applying the transformation, $\varsigma = \rho v - Qu - Q'\omega + \eta\vartheta + \eta\sum_{j=1}^{r} b_j x_{1-j} + \eta\varepsilon_1$, and $c = \frac{\varsigma-\rho v+Qu+Q'\omega}{\eta} - \vartheta - \sum_{j=1}^{r} b_j x_{1-j}$, then $dc = \frac{1}{\eta}d\varsigma$. Hence, the integral equation becomes

$$\Pi(v) = 1 + \frac{1}{\eta}\int_L^H \Pi(\varsigma) f\left(\frac{\varsigma - \rho v + Qu + Q'\omega}{\eta} - \vartheta - \sum_{j=1}^{r} b_j x_{1-j}\right) d\varsigma \tag{8}$$

Next, we establish the existence and uniqueness of the solution; the detailed proof is omitted here and provided in the Appendix B.

Step 4: Explicit ARL under exponential white noise. Assume that $\varepsilon_1 \sim \text{Exp}(\alpha)$. Then,

$$\Pi(v) = 1 + \frac{1}{\eta\alpha}\exp\left(\frac{\rho v - Qu - Q'\omega}{\eta\alpha} + \frac{\vartheta + \sum_{j=1}^{r} b_j x_{1-j}}{\alpha}\right)\int_L^H \Pi(\varsigma)\exp\left(-\frac{\varsigma}{\eta\alpha}\right)d\varsigma.$$

Next, set $M = \int_L^H \Pi(\varsigma)\exp\left(-\frac{\varsigma}{\eta\alpha}\right)d\varsigma$ and $N(v) = \exp\left(\frac{\rho v-Qu-Q'\omega}{\eta\alpha} + \frac{\vartheta+\sum_{j=1}^{r} b_j x_{1-j}}{\alpha}\right)$, thus yielding in (9)

$$\Pi(v) = 1 + \frac{M \cdot N(v)}{\eta\alpha}. \tag{9}$$

Step 5: Determination of the constant M. Next, the constant M is obtained by integrating $\Pi(v)$ over the interval $[L, H]$. Thus,

$$M = \int_L^H \Pi(\varsigma)\exp\left(-\frac{\varsigma}{\eta\alpha}\right)d\varsigma = \int_L^H \left[1 + \frac{M \cdot N(\varsigma)}{\eta\alpha}\right]\exp\left(-\frac{\varsigma}{\eta\alpha}\right)d\varsigma.$$

After simplification, we obtain

$$M = \frac{-\eta\alpha\left[\exp\left(-\frac{H}{\eta\alpha}\right) - \exp\left(-\frac{L}{\eta\alpha}\right)\right]}{1 + \frac{1}{\lambda_2}\exp\left(\frac{-Qu-Q'\omega}{\eta\alpha} + \frac{\vartheta+\sum_{j=1}^{r} b_j x_{1-j}}{\alpha}\right)\left[\exp\left(-\frac{H}{\eta\alpha}\right) - \exp\left(-\frac{L}{\eta\alpha}\right)\right]}.$$

Let $M_0(\varsigma) = \exp\left(-\frac{\varsigma}{\eta\alpha}\right)$; it follows from Equation (10) that

$$M = \frac{-\eta\alpha[M_0(H) - M_0(L)]}{1 + \frac{1}{\lambda_2}\exp\left(\frac{-Qu-Q'\omega}{\eta\alpha} + \frac{\vartheta+\sum_{j=1}^{r} b_j x_{1-j}}{\alpha}\right)[M_0(H) - M_0(L)]}. \tag{10}$$

Step 6: Explicit closed-form ARL solution. Substituting Equation (10) into Equation (9), the explicit ARL of the double-modified EWMA chart under the ARX(p, r) model is obtained as

$$\Pi(v) = 1 - \frac{\lambda_2 \exp\left(\frac{\rho v}{\eta\alpha}\right)[M_0(H) - M_0(L)]}{[M_0(\lambda_2 H) - M_0(\lambda_2 L)] + \lambda_2 M_0[-Qu - Q'\omega]M_0\left[\eta(\vartheta + \sum_{j=1}^{r} b_j x_{1-j})\right]}. \tag{11}$$

From Equation (11), let $\Pi(v)$ denote the explicit closed-form solution of ARL, and it had notation that was shown as $\mathrm{ARL}_{\text{1-sided}}$ and $\mathrm{ARL}_{\text{2-sided}}$ for asymmetric one-sided and symmetric two-sided double-modified EWMA charts when L equals 0 and is greater than 0, respectively. Consequently, the ARL for the symmetric two-sided double-modified EWMA chart under the ARX(p, r) process is given by

$$\mathrm{ARL}_{\text{2-sided}} = 1 - \frac{\lambda_2 \exp\left(\frac{\rho v}{\eta\alpha}\right)[M_0(H) - M_0(L)]}{[M_0(\lambda_2 H) - M_0(\lambda_2 L)] + \lambda_2 M_0[-Qu - Q'\omega]M_0\left[\eta(\vartheta + \sum_{j=1}^{r} b_j x_{1-j})\right]},$$

Similarly, the one-sided chart is expressed as

$$\mathrm{ARL}_{\text{1-sided}} = 1 - \frac{\lambda_2 \exp\left(\frac{\rho v}{\eta\alpha}\right)[M_0(H) - 1]}{[M_0(\lambda_2 H) - 1] + \lambda_2 M_0[-Qu - Q'\omega]M_0\left[\eta(\vartheta + \sum_{j=1}^{r} b_j x_{1-j})\right]}.$$

where α is represented by α_0 and α_1, and the function $M_0(\varsigma)$ is denoted according to the controllable and uncontrollable cases as follows:

$$M_0(\varsigma) = \exp\left(-\frac{\varsigma}{\eta\alpha_0}\right) \quad \text{and} \quad M_0(\varsigma) = \exp\left(-\frac{\varsigma}{\eta\alpha_1}\right).$$

3.1.2. Steps of Deriving the ARL Solution by NIE Method Under ARX(p, r) Model

The NIE method with quadrature is used to accurately approximate the ARL of the double-modified EWMA control chart for the ARX(p, r) process with exponential white noise. The procedure is summarized as follows.

Step 1: Discretization of the monitoring interval.

Let $\Pi'(v)$ denote the ARL function of the double-modified EWMA control chart under the ARX(p, r) model. The monitoring interval $[L, H]$ is divided into n subintervals. The quadrature nodes and weights are defined by $w_j = \frac{H-L}{n}$, and $\varpi_j = L + (j - 0.5)w_j$, $j = 1, 2, \ldots, n$. Using the quadrature approximation, the integral term can be written as $\int_L^H f(v)\,dv \approx \sum_{j=1}^{n} w_j f(\varpi_j)$.

Step 2: Approximation of the ARL integral equation.

Applying the quadrature rule to the NIE formulation gives the ARL values at the grid points as

$$\Pi'(\varpi_i) = 1 + \frac{1}{\eta}\sum_{j=1}^{n} w_j \Pi'(\varpi_j) f\left(\frac{\varpi_j - \rho v + Qu + Q'\omega}{\eta} - \vartheta - \sum_{j=1}^{r} b_j x_{1-j}\right), i = 1, 2, \ldots, n.$$

Step 3: Matrix representation. The equation in Step 2 above yields a system of n linear equations, which can be expressed in matrix form as $\mathbf{M} = (\mathbf{I} - \mathbf{R})^{-1}\mathbf{1}$, where $\mathbf{M} = \left(\Pi'(\varpi_1), \Pi'(\varpi_2), \ldots, \Pi'(\varpi_n)\right)^{\top}, \mathbf{1} = (1, 1, \ldots, 1)^{\top}, \mathbf{I} = \text{diag}(1, 1, \ldots, 1)$, and the $(i, j)^{th}$ element of $\mathbf{R}$ is $R_{ij} = \frac{w_j}{\eta} f\left(\frac{\varpi_j - \rho v + Qu + Q'\omega}{\eta} - \vartheta - \sum_{j=1}^{r} b_j x_{1-j}\right)$.

Step 4: Evaluation at an initial value.

After solving the linear system, the ARL at an initial value v is computed by replacing r_i with v:

$$\Pi'(v) = 1 + \frac{1}{\eta}\sum_{j=1}^{n} w_j \Pi'(\varpi_j) f\left(\frac{\varpi_j - \rho v + Qu + Q'\omega}{\eta} - \vartheta - \sum_{k=1}^{r} b_k x_{1-k}\right). \tag{12}$$

Therefore, Equation (12) represents the NIE-based numerical approximation of the ARL function for DMEWMA chart under the ARX(p, r) model.

3.2. ARL Derivation Under an ARFI Model with Exogenous Variables

The ARL expressions obtained from the explicit closed-form formula and the NIE method are presented under the ARFIX(p, d, r) framework. The ARFIX(p, d, r) model, or autoregressive fractionally integrated model with exogenous variables, extends the ARX(p, r) model by incorporating the fractional differencing parameter d. This additional parameter enables the model to capture long-memory dependence. Hence, in addition to autoregressive effects and exogenous variables, the ARFIX model also describes fractional integration behavior.

3.2.1. Steps of Deriving the Explicit Closed-Form ARL Solution Under the ARFIX(p, d, r) Model

In this subsection, the ARFIX(p, d, r) model is used to derive the explicit closed-form ARL solution. The model is obtained by adding the fractional differencing operator $(1 - B)^d$ to the ARX(p, r) structure. Using Equations (2) and (3), the ARFIX(p, d, r) model can be conveniently reformulated in a compact form.

$$z_t = \vartheta + \varepsilon_t + \sum_{j=1}^{r} b_j x_{1-j} + \left(d z_{t-1} - \frac{d(d-1)}{2!} z_{t-2} + \frac{d(d-1)(d-2)}{3!} z_{t-3} - \cdots\right)$$
$$+ \sum_{i=1}^{p}\left(\phi_i z_{t-i} - d\phi_i z_{t-(i+1)} + \frac{d(d-1)}{2!}\phi_i z_{t-(i+2)} - \frac{d(d-1)(d-2)}{3!}\phi_i z_{t-(i+3)} + \cdots\right),$$

Here, $z_{t-1}, z_{t-2}, \ldots$ denote lagged observations, while $0 < d < 0.5$ indicates stationary long-memory behavior.

Step 1: Substitution into the double-modified EWMA statistic. Substituting z_t into the double-modified EWMA statistic in Equation (6), at $t = 1$, let $\Psi_0 = v$, $\Xi_0 = u$, and $z_0 = \omega$. Then,

$$\begin{aligned}\Psi_1 = (1-\lambda_2)v - (\lambda_1\lambda_2 + \lambda_1\kappa_2 - \lambda_2)u - (\kappa_1\lambda_2 + \kappa_1\kappa_2)\omega \\ + \eta\left[\vartheta + \varepsilon_1 + \sum_{j=1}^{r} b_j x_{1-j} + dz_0 - \frac{d(d-1)}{2!}z_{-1} + \cdots \right. \\ \left. + \sum_{i=1}^{p}\left(\phi_i z_{1-i} - d\phi_i z_{-i} + \frac{d(d-1)}{2!}\phi_i z_{-(i+1)} - \cdots\right)\right].\end{aligned} \tag{13}$$

For simplicity, define

$$F = dz_0 - \frac{d(d-1)}{2!}z_{-1} + \cdots + \sum_{i=1}^{p}\left(\phi_i z_{1-i} - d\phi_i z_{-i} + \frac{d(d-1)}{2!}\phi_i z_{-(i+1)} - \cdots\right).$$

Thus, Ψ_1 becomes

$$(1-\lambda_2)v - (\lambda_1\lambda_2 + \lambda_1\kappa_2 - \lambda_2)u - (\kappa_1\lambda_2 + \kappa_1\kappa_2)\omega + \eta\left[\vartheta + \varepsilon_1 + \sum_{j=1}^{r} b_j x_{1-j} + F\right].$$

Adding the fractional component F to the subsequent control period in Step 2 of Section 3.1.1 transforms it into

$$l' < (1-\lambda_2)v - (\lambda_1\lambda_2 + \lambda_1\kappa_2 - \lambda_2)u - (\kappa_1\lambda_2 + \kappa_1\kappa_2)\omega + \eta\vartheta + \eta\sum_{j=1}^{r} b_j x_{1-j} + \eta F + \eta\varepsilon_1 < h'.$$

Following Steps 2–6 in Section 3.1.1, the derivation proceeds in the same manner as in the ARX case. Let $\Omega(v)$ denote the additional fractional component of the ARFIX(p,d,r) model. Then, the explicit closed-form ARL under the ARFIX(p,d,r) model is obtained as

$$\Omega(v) = 1 - \frac{\lambda_2 \exp\left(\frac{\rho v}{\eta\alpha}\right)[M_0(H') - M_0(L')]}{[M_0(\lambda_2 H') - M_0(\lambda_2 L')] + \lambda_2 M_0[-Qu - Q'\omega]M_0\left[\eta(\vartheta + \sum_{j=1}^{r} b_j x_{1-j} + F)\right]}. \tag{14}$$

When L' is equal to 0, the explicit closed-form solution of ARL is shown as $\text{ARL}_{\text{1-sided}}$, and when L' is greater than 0, it is shown as $\text{ARL}_{\text{2-sided}}$. These notations stand for asymmetric one-sided and symmetric two-sided double-modified EWMA charts, respectively. Hence, the ARFIX(p,d,r) process's ARL for the symmetric two-sided double-modified EWMA chart may be expressed as

$$\text{ARL}_{\text{2-sided}} = 1 - \frac{\lambda_2 \exp\left(\frac{\rho v}{\eta\alpha}\right)[M_0(H') - M_0(L')]}{[M_0(\lambda_2 H') - M_0(\lambda_2 L')] + \lambda_2 M_0(-Qu - Q'\omega)M_0\left(\eta\left(\vartheta + \sum_{j=1}^{r} b_j x_{1-j} + F\right)\right)}.$$

For the one-sided chart, the corresponding ARL is given by

$$\text{ARL}_{\text{1-sided}} = 1 - \frac{\lambda_2 \exp\left(\frac{\rho v}{\eta\alpha}\right)[M_0(H') - 1]}{[M_0(\lambda_2 H') - 1] + \lambda_2 M_0(-Qu - Q'\omega)M_0\left(\eta\left(\vartheta + \sum_{j=1}^{r} b_j x_{1-j} + F\right)\right)}.$$

3.2.2. ARL for the ARFIX(p,d,r) Model Using the Numerical Integral Equation

In this subsection, the NIE method is applied to approximate the ARL of the double-modified EWMA control chart under the ARFIX(p,d,r) model.

Following the same procedure as in Section 3.1.2, the ARL is evaluated from the integral equation using the Gauss–Legendre quadrature rule. It can be shown as

$$\Omega(v) = 1 + \frac{1}{\eta}\int_{L'}^{H'} \Pi(\varsigma)\left(\frac{\varsigma - \rho v + Qu + Q'\omega}{\eta} - \vartheta - \sum_{j=1}^{r} b_j x_{1-j} - F\right) d\varsigma \tag{15}$$

Let $\Omega'(v)$ be ARL for the ARFIX(p,d,r) model using the NIE technique,

$$\Omega'(v) = 1 + \frac{1}{\eta}\sum_{j=1}^{n} w_j \Pi'(\varpi_j) f\left(\frac{r_j - \rho v + Qu + Q'\omega}{\eta} - \vartheta - \sum_{j=1}^{r} b_j x_{1-j} - F\right). \tag{16}$$

3.3. Algorithm for Computing the Closed-Form Expression for Run-Length Evaluation

Algorithm 1 summarizes the results of the explicit closed-form ARL calculation and the derivation of the control chart coefficients for the double-modified EWMA chart using the ARX and ARFIX models.

Algorithm 1: Algorithm for computing the explicit closed-form expression for ARL of the double-modified EWMA chart under ARX(p,r) and ARFIX(p,d,r) frameworks.

Purpose: In order to find the related control chart coefficients for the double-modified EWMA control chart under ARX(p,r) and ARFIX(p,d,r) processes with exponential white noise and to calculate the explicit closed-form ARL.

Input specifications:

1. Specify ϑ, ϕ_i, b_j, and x_{1-j} for the ARX model. For the ARFIX model, include the fractional differencing parameter d, where $0 < d < 0.5$, to account for long-memory dependence.
2. Define the DMEWMA chart parameters: $\lambda_2 = 0.05, 0.10, 0.15$, $\lambda_1 = 2\lambda_2$, and $\kappa_1, \kappa_2 \in \{1, 3, 9\}$.
3. Set the in-control exponential mean parameter as $\alpha_0 = 1$ with the target $\text{ARL}_0 = 370$.
4. Set the out-of-control exponential mean parameter as $\alpha_1 = (1+\delta)\alpha_0$, where δ denotes the shift size and $\delta = 0.001, 0.0025, 0.005, 0.01, 0.025, 0.1, 0.25, 0.5$.

Computational steps:

Step 1: Model construction.
Define the ARX(p,r) and ARFIX(p,d,r), denoted by y_t and z_t, respectively, under exponential white noise. Assign all initial values and model coefficients.

Step 2: In-control setting.
Set $\alpha = \alpha_0$ to represent the in-control process. Then specify the control limit structure: LCL$= 0$ for the one-sided chart and LCL$= 0.1, 0.4$ for the symmetric two-sided chart.

Step 3: Computation of the upper control limit.
For each combination of λ, r_1, and r_2, find the corresponding UCL such that the in-control ARL satisfies the target value $\text{ARL}_0 \approx 370$.

Step 4: Out-of-control ARL evaluation.
For each shift size δ, define the shifted mean parameter as $\alpha = \alpha_1 = (1+\delta)\alpha_0$. The corresponding UCL values are then used to compute ARL_1 based on the explicit closed-form formula.

Step 5: ARL computation.
The ARL_1 values computed from the explicit closed-form formula in Step 4 are compared with the corresponding NIE results.

Output:
The procedure provides the calibrated upper control limits, and the ARL_1 values computed from the explicit closed-form formula, for the ARX(p,r) and ARFIX(p,d,r) models.

4. Performance Measures

4.1. Validation of Explicit Closed-Form ARL Against NIE

To validate the explicit closed-form ARL results, the ARL values obtained from the explicit closed-form formula are compared with those computed using the NIE method. The percentage relative change, denoted by $\%RPC$, is defined as

$$\%RPC_{ARX} = \left| \frac{\Pi(v) - \Pi'(v)}{\Pi(v)} \right| \times 100. \tag{17}$$

and

$$\%RPC_{ARFIX} = \left| \frac{\Omega(v) - \Omega'(v)}{\Omega(v)} \right| \times 100. \tag{18}$$

where $\%RPC_{\mathrm{ARX}}$ and $\%RPC_{\mathrm{ARFIX}}$ denote the percentage relative changes between the explicit ARL and the NIE-based ARL for the ARX and ARFIX models, respectively.

4.2. Run-Length Performance Measures

The SDRL is considered together with the ARL to evaluate the detection performance and run-length stability of a control chart [26]. The ARL indicates the expected time to signal, whereas the SDRL measures the variability of the run length. Thus, smaller ARL_1 and SDRL_1 values imply faster and more stable detection of out-of-control shifts.

The in-control and out-of-control ARL and SDRL values are calculated by

$$\begin{aligned} &\text{In control:} && \mathrm{ARL}_0 = \beta^{-1}, && \mathrm{SDRL}_0 = \frac{\sqrt{1-\beta}}{\beta}, \\ &\text{Out of control:} && \mathrm{ARL}_1 = (1-\nu)^{-1}, && \mathrm{SDRL}_1 = \frac{\sqrt{\nu}}{1-\nu}. \end{aligned} \tag{19}$$

where $\mathrm{ARL}_0 = 370$. The out-of-control performance is better for smaller values of ARL_1 and SDRL_1. The smaller the ARL_1, the fewer observations the chart needs to detect a shift in the process. The smaller the SDRL_1, the less variation in the detection time. Hence, a chart with small ARL_1 and SDRL_1 can detect the shifts faster and more reliably. For the symmetric two-sided chart, the ARL is computed for symmetric lower and upper control limits so that shifts in both upward and downward directions can be detected with equal sensitivity. Hence, symmetry adds to equal detection performance on both sides of the target process level.

4.3. Comparative Performance Indices for Control Charts

Next, an additional measurement of how effectively various control charts identify faults is made using the relative mean index (RMI) [26]. It quantifies the average relative deviation of the ARL_1 value of a given chart from the smallest ARL_1 value obtained at each shift level. The RMI is defined as

$$\mathrm{RMI} = \frac{1}{\Delta} \sum_{j=1}^{\Delta} \left| \frac{\mathrm{ARL}_1(\delta_j) - \mathrm{ARL}_1'(\delta_j)}{\mathrm{ARL}_1'(\delta_j)} \right|, \tag{20}$$

where Δ is the total number of mean shift values, $\mathrm{ARL}_1(\delta_i)$ denotes the out-of-control ARL at shift size δ_i, and $\mathrm{ARL}_1'(\delta_j)$ is the minimum ARL_1 value among all charts compared at the same shift size. A smaller RMI value indicates better detection performance, as the chart is closer to the best-performing chart at each shift level. The minimum value of RMI is 0, indicating the best possible relative performance.

Similarly, the relative standard deviation index (RSDI) is used to compare the stability of the run length among competing charts based on SDRL_1. A lower RSDI value indicates

that the chart has an $SDRL_1$ close to the smallest $SDRL_1$ among all charts. Therefore, an RSDI value close to zero implies more stable and consistent detection performance. The RSDI is calculated as

$$\text{RSDI} = \frac{1}{\Delta}\sum_{i=1}^{\Delta}\left|\frac{\text{SDRL}_1(\delta_i) - \text{SDRL}_1'(\delta_i)}{\text{SDRL}_1'(\delta_i)}\right|. \tag{21}$$

where $SDRL_1(\delta_i)$ represents the out-of-control SDRL at shift size δ_i, and $SDRL_1'(\delta_i)$ is the minimum $SDRL_1$ value among all charts compared at the same shift size.

5. Results and Discussion

5.1. Numerical Validation

The detection ability and practical efficiency of control charts in the case of process mean shifts are commonly evaluated by the average run length (ARL) as the primary criterion. In this work, the explicit closed-form solution and the numerical integral equation (NIE) approach are employed to evaluate the ARL performance of the double-modified EWMA control chart for detecting the mean changes in ARX(p,r) and ARFIX(p,d,r) models with exponential white noise. The control limit is selected so that the average run length when the process is in control is approximately $ARL_0 = 370$. We set $\alpha_0 = 1$ for the initial mean parameter. For the numerical implementation, the NIE method is implemented with $m = 500$ subintervals to approximate the ARL values.

The process is assumed to follow exponential white noise with mean $\alpha_0 = 1$ under the in-control state. This setting provides a stable baseline to evaluate the symmetry and detection performance of the proposed control chart. Symmetry is discussed in the context of process monitoring in terms of the chart's ability to respond to changes in process structure in a consistent manner while maintaining the desired in-control performance. At a process shift the mean changes from α_0 to α_1, with $\alpha_1 = (1+\delta)\alpha_0$. The case $\delta = 0$ represents the in-control condition, corresponding to ARL_0, whereas $\delta > 0$ indicates the out-of-control condition, corresponding to ARL_1. The ARL data are used to evaluate the ability of the control chart to detect mean changes in various magnitudes.

Table 1 reports a comparison of ARL values for the double-modified EWMA control chart under the ARX(p,r) and ARFIX(p,d,r) models, computed using both the explicit closed-form expression and the numerical integral equation (NIE) method. The control limit is determined so that the in-control average run length is approximately $ARL_0 = 370$. For the ARX(p,r) model, the parameters are set as $\lambda = \lambda_2 = 0.10$, $\lambda_1 = 2\lambda_2$, $\vartheta = 1.5$, $b_1 = 0.75$, and $b_2 = 0.5$, whereas for the ARFIX(p,d,r) model, the corresponding settings are $\lambda = \lambda_2 = 0.15$, $\lambda_1 = 2\lambda_2$, $\vartheta = 2$, and $b_1 = b_2 = 0.5$. The numerical computations were carried out on a Windows 10 64-bit computer equipped with an Intel Core i5-8250U processor operating at 1.60–1.80 GHz and 4 GB of RAM.

As shown in Table 1, the ARL values obtained from the explicit closed-form formulas are almost identical to those computed using the NIE method for all considered ARX(p,r) and ARFIX(p,d,r) models. In Table 1, the cases with $LCL = 0$ correspond to one-sided control schemes, whereas those with $LCL = 0.1$ correspond to two-sided control schemes. The close agreement between the explicit closed-form and NIE results is observed under both one-sided and two-sided cases, as well as under positive and negative autoregressive parameter settings, indicating that the proposed explicit closed-form formulas provide highly accurate ARL approximations.

The ARL values decline greatly for all model parameters when the shift size δ rises. This pattern shows that the double-modified EWMA control chart responds more rapidly to larger process shifts. For the ARX$(1,1)$ model with $\phi_1 = 0.2$, the ARL values exhibit a clear decreasing trend as the shift size δ increases.

Table 1. Comparison of ARL values under the ARX(p,r) and ARFIX(p,d,r) models using explicit closed-form and NIE methods running on the double-modified EWMA control chart, with parameters ARX ($\lambda = 0.1$, $\vartheta = 1.5$, $b_1 = 0.75$, and $b_2 = 0.5$); ARFIX ($\lambda = 0.15$, $\vartheta = 2$, and $b_1 = b_2 = 0.5$), when determined ARL_0 equals 370.

Model	**LCL**	ϕ_1	$\phi_1 = 0.2$				$\phi_1 = -0.2$			
		UCL	$H = 0.174372$				$H = 0.261022$			
		δ	$\Pi(v)$	$\Pi'(v)$	**Time**	%RPC	$\Pi(v)$	$\Pi'(v)$	**Time**	%RPC
ARX(1, 1)	0	0	370.32354557	370.32354237	1.453	8.65×10^{-7}	370.22471607	370.22470877	1.485	1.97×10^{-6}
		0.001	231.48071319	231.48071169	1.531	6.46×10^{-7}	241.25190343	241.25189980	1.5	1.51×10^{-6}
		0.0025	148.20315062	148.20314986	1.39	5.15×10^{-7}	158.50201731	158.50201540	1.515	1.21×10^{-6}
		0.005	92.697804727	92.697804333	1.577	4.25×10^{-7}	100.90339880	100.90339780	1.454	9.92×10^{-6}
		0.01	53.060357515	53.060357325	1.579	3.58×10^{-7}	58.504451303	58.504450818	1.562	8.28×10^{-6}
		0.025	23.347873326	23.347873257	1.422	2.97×10^{-7}	25.999390785	25.999390608	1.469	6.80×10^{-6}
		0.1	6.3665622501	6.3665622368	1.485	2.09×10^{-7}	7.1233802072	7.1233801730	1.469	4.80×10^{-6}
		0.25	2.8675173193	2.8675173158	1.485	1.23×10^{-7}	3.1873349355	3.1873349263	1.562	2.90×10^{-6}
		0.5	1.7747290986	1.7747290976	1.453	5.67×10^{-8}	1.9385202364	1.9385202336	1.485	1.41×10^{-7}
Model	LCL	ϕ_1, ϕ_2	$\phi_1 = 0.2, \phi_2 = 0.6$				$\phi_1 = 0.2, \phi_2 = -0.6$			
		UCL	$H = 0.19616$				$H = 0.422112$			
		δ	$\Pi(v)$	$\Pi'(v)$	Time	%RPC	$\Pi(v)$	$\Pi'(v)$	Time	%RPC
ARX(2, 2)	0.1	0	370.13550972	370.13550872	1.5	2.70×10^{-7}	370.31889603	370.31888421	1.5	3.19×10^{-6}
		0.001	211.74347133	211.74347092	1.484	1.92×10^{-7}	240.97437222	240.97436641	1.453	2.41×10^{-6}
		0.0025	129.02715389	129.02715369	1.453	1.50×10^{-7}	158.20155227	158.20154924	1.516	1.91×10^{-6}
		0.005	78.211646158	78.211646062	1.453	1.24×10^{-7}	100.68587605	100.68587448	1.406	1.56×10^{-6}
		0.01	43.828671659	43.828671613	1.454	1.05×10^{-7}	58.399236950	58.399236197	1.499	1.29×10^{-6}
		0.025	19.027286914	19.027286897	1.563	8.79×10^{-8}	26.007769207	26.007768935	1.453	1.05×10^{-6}
		0.1	5.2197860036	5.2197860004	1.454	6.06×10^{-8}	7.1978077304	7.1978076775	1.515	7.34×10^{-7}
		0.25	2.4226227038	2.4226227029	1.5	3.35×10^{-8}	3.2593820384	3.2593820239	1.469	4.47×10^{-7}
		0.5	1.5658690030	1.5658690027	1.547	1.43×10^{-8}	1.9951163683	1.9951163639	1.516	2.22×10^{-7}
Model	LCL	ϕ_1	$\phi_1 = 0.3$				$\phi_1 = -0.3$			
		UCL	$H' = 0.096462$				$H' = 0.131501$			
		δ	$\Omega(v)$	$\Omega'(v)$	Time	%RPC	$\Omega(v)$	$\Omega'(v)$	Time	%RPC
ARFIX(1, 0.25, 1)	0	0	370.19091576	370.19091426	2.593	4.04×10^{-7}	370.17515356	370.17515076	2.75	7.56×10^{-7}
		0.001	205.16764266	205.16764214	2.656	2.53×10^{-7}	212.14917872	212.14917769	2.781	4.86×10^{-7}
		0.0025	123.03245507	123.03245485	2.626	1.78×10^{-7}	129.41251142	129.41251097	2.75	3.44×10^{-7}
		0.005	73.872497790	73.872497692	2.562	1.33×10^{-7}	78.512141604	78.512141403	2.75	2.56×10^{-7}
		0.01	41.152292098	41.152292056	2.672	1.01×10^{-7}	44.040096275	44.040096190	2.813	1.94×10^{-7}
		0.025	17.816528054	17.816528041	2.797	7.62×10^{-8}	19.157312301	19.157312273	2.796	1.45×10^{-7}
		0.1	4.9206367308	4.9206367284	2.796	4.82×10^{-8}	5.2912308283	5.2912308234	2.75	9.16×10^{-8}
		0.25	2.3171899531	2.3171899525	2.765	2.57×10^{-8}	2.4708373226	2.4708373213	2.765	5.02×10^{-8}
		0.5	1.5213736873	1.5213736871	2.734	1.07×10^{-8}	1.5979884259	1.5979884256	2.75	2.16×10^{-8}
Model	LCL	ϕ_1, ϕ_2	$\phi_1 = 0.3, \phi_2 = 0.5$				$\phi_1 = 0.3, \phi_2 = -0.5$			
		UCL	$H' = 0.1753115$				$H' = 0.226177$			
		δ	$\Omega(v)$	$\Omega'(v)$	Time	%RPC	$\Omega(v)$	$\Omega'(v)$	Time	%RPC
ARFIX(2, 0.45, 2)	0.1	0	370.30173910	370.30173815	2.859	2.57×10^{-7}	370.29927942	370.29927672	2.875	7.29×10^{-7}
		0.001	194.66714814	194.66714784	2.797	1.54×10^{-7}	206.10214460	206.10214366	2.844	4.56×10^{-7}
		0.0025	113.84384490	113.84384477	2.781	1.07×10^{-7}	123.87600514	123.87600474	2.812	3.19×10^{-7}
		0.005	67.378706370	67.378706316	2.859	7.91×10^{-8}	74.500554589	74.500554413	2.796	2.35×10^{-7}
		0.01	37.206181167	37.206181144	2.828	6.06×10^{-8}	41.569331036	41.569330962	2.766	1.78×10^{-7}
		0.025	16.044475116	16.044475108	2.86	4.57×10^{-8}	18.048343276	18.048343252	2.765	1.32×10^{-7}
		0.1	4.4770960830	4.4770960817	2.812	2.85×10^{-8}	5.0286172629	5.0286172587	2.766	8.32×10^{-8}
		0.25	2.1562472136	2.1562472133	2.952	1.48×10^{-8}	2.3851105983	2.3851105972	2.78	4.51×10^{-8}
		0.5	1.4511794391	1.4511794390	2.859	5.89×10^{-9}	1.5653237103	1.5653237100	2.921	1.92×10^{-8}

A similar pattern is found for the ARX$(2,2)$, ARFIX$(1, 0.25, 1)$, and ARFIX$(2, 0.45, 2)$ models, indicating consistent detection behavior across all considered model settings.

The very small %RPC values indicate that the explicit closed-form formulas produce ARL values that are nearly identical to those obtained from the NIE method. However, the explicit closed-form approach is much more computationally efficient, requiring less than 0.001 s, compared with less than 1.6 s for the ARX models and less than 3 s for the more complex ARFIX models using the NIE method. Therefore, the explicit closed-form ARL formulas are preferred because they achieve comparable numerical accuracy with substantially lower computational cost.

5.2. Explicit Closed-Form Solution and NIE Technique with Computing Efficiency and Complexity

The explicit closed-form solution for ARL has the advantage of computational efficiency, as the ARL value can be obtained directly once the model parameters and control limits are specified. The closed-form expression does not require repeated numerical integration as in the NIE method that requires discretization of the monitoring interval and solution of a system of linear equations. The proposed explicit formula thus reduces computational burden, especially when ARL values have to be evaluated repeatedly for different shift sizes, smoothing parameters, or control-limit settings. However, for more complex models such as ARFIX, the fractional integration component creates long-memory dependence that can increase the computational effort to evaluate the model terms.

5.3. Simulated Data Analysis

To evaluate the performance of the EWMA, modified EWMA, and double-modified EWMA control charts under the ARX(p, r) and ARFIX(p, d, r) models, the simulated data analysis is presented in this part. An evaluation of the detection capability, run-length variability, and overall relative performance of the competing control charts is based on the relative mean index (RMI), standard deviation of run length (SDRL), and average run length (ARL). The explicit closed-form solution, which is derived from simulation data, is used to calculate all ARL and SDRL values. Specifically, the key value of the clear closed formula, ARL, from simulation data analysis, is that a lower ARL indicates that the process is out of control. This shows that the control chart can detect process changes more quickly. Therefore, the proposed DMEWMA chart exhibits better sensitivity in detecting changes than other EWMA chart types when providing a lower ARL. From a practical perspective, a reduction in ARL means that out-of-control conditions can be signaled more quickly, and thus, corrective actions can be taken more rapidly.

The competing charts considered in this study consist of the conventional EWMA chart, the modified EWMA chart with $\kappa = 1$, and the double-modified EWMA chart with four parameter settings, namely $(\kappa_1, \kappa_2) = (1,1)$, $(1,3)$, $(1,9)$, and $(3,9)$. The smoothing parameters are specified as $\lambda = \lambda_2 = 0.05$, 0.10, and 0.15, while the corresponding values of λ_1 are set to 0.10, 0.20, and 0.30, respectively, so that $\lambda_1 = 2\lambda_2$ in all cases. In addition, the parameters of the exogenous variable x_t are fixed as $b_1 = b_2 = 1$ throughout the simulation study. For comparison purposes, the behavior of the competing charts for $\lambda = 0.05$, 0.10, and 0.20 is also shown in Figures A1–A4.

A comparison of the results of the EWMA, modified EWMA and double-modified EWMA control charts under the ARX model is shown in Tables A1–A4. The control limits $[0, \text{UCL}]$ in Table A1 are for the one-sided monitoring system based on the ARX$(p, 1)$ model with parameters $\vartheta = 1$, $\phi_1 = 0.1$, and $\phi_2 = 0.4$. Tables A3 and A4 are comparable to the two-sided monitoring scheme under the ARX$(p, 2)$ model with control limits $[\text{LCL}, \text{UCL}]$ set at 0.1 and 0.4. Tables A3 and A4 are for the two-sided monitoring framework with control limits at $[\text{LCL}, \text{UCL}]$ under the ARX$(p, 2)$ model, for LCL $= 0.1$ and 0.4. The parameters are specified as $\vartheta = 0$, $\phi_1 = \phi_2 = 0.2$ and $\phi_3 = 0.3$. In each example, the corresponding higher control limit is chosen such that $\text{ARL}_0 = 370$.

The values of ARL_1 for the modified EWMA and double-modified EWMA control charts are generally smaller than those of the conventional EWMA chart as shown in Tables A1–A4, especially for small and moderate shift levels. Among the competing charts, the double-modified EWMA chart provides the most competitive performance across the considered shift levels. As the shift size δ increases, the ARL_1 values decrease for all charts, indicating faster detection of larger process shifts. The SDRL_1 results follow a similar decreasing trend, indicating that the detection performance tends to be more stable as the shift magnitude increases. These patterns can also be clearly seen in Figure A1, which

shows the variation in ARL_1 and $SDRL_1$ with respect to δ under the ARX(p, r) model for the EWMA, modified EWMA, and double-modified EWMA charts with $(\kappa_1, \kappa_2) = (1, 1)$, $(1, 3)$, $(1, 9)$, and $(3, 9)$.

Figure A2 also shows the corresponding RMI and RSDI values under the ARX(p, r) model. The RMI measures the relative difference between the ARL_1 value of each chart and the smallest ARL_1 value at each shift level, while the RSDI measures the relative difference between the $SDRL_1$ value and the smallest $SDRL_1$ value at the same shift level. Smaller RMI and RSDI values indicate better overall performance, with values close to zero showing that the chart performs close to the best-performing chart across the considered shift levels. The graphical results in Figure A2 support the tabulated results by showing that the double-modified EWMA chart generally attains the smallest or near-smallest RMI and RSDI values under the ARX(p, r) model.

Tables A5–A8 present the comparative performance of the EWMA, modified EWMA, and double-modified EWMA control charts under the ARFIX model. Tables A5 and A6 corresponds to the one-sided monitoring scheme with control limits set at $[0, \text{UCL}]$ under the ARFIX$(1, d, 1)$ model, where $d = 0.25$ and 0.45 are considered. The lower control limit is fixed at $\text{LCL} = 0$, and the parameters are specified as $\vartheta = 0.9$ and $\phi_1 = 0.2$. Tables A7 and A8 corresponds to the two-sided monitoring scheme with control limits set at $[\text{LCL}, \text{UCL}]$ under the ARFIX$(2, d, 2)$ model, where $d = 0.25$ and 0.45 are considered. The lower control limit is fixed at $\text{LCL} = 0.1$, and the parameters are specified as $\vartheta = 2$, $\phi_1 = 0.2$, and $\phi_2 = 0.4$. For each ARFIX case, the corresponding upper control limit is determined such that $ARL_0 = 370$.

The results in Tables A5–A8 indicate that the double-modified EWMA control chart remains effective under fractionally integrated autoregressive models. Compared with the conventional EWMA chart, the modified EWMA and double-modified EWMA charts generally produce smaller ARL_1 values, indicating greater sensitivity in detecting process mean shifts. The double-modified EWMA chart shows particularly strong performance across the considered shift magnitudes and fractional differencing parameters. The $SDRL_1$ values show the same pattern as the ARL_1 values, which confirms that the proposed chart provides faster detection and more consistent run-length behavior. These relationships are depicted in Figure A3, which displays the change in ARL_1 and $SDRL_1$ with the shift magnitude δ under the ARFIX(p, d, r) model for the EWMA, modified EWMA, and double-modified EWMA control charts. The values of RMI and RSDI for the ARFIX(p, d, r) model are presented in Figure A4. Again, the graphical results show that the double-modified EWMA chart generally has the lowest or near the lowest values of RMI and RSDI among the cases considered. This evidence is consistent with the tabulated ARL_1 and $SDRL_1$ results and further supports the overall superiority of the double-modified EWMA chart under ARFIX model settings.

Moreover, double-modified EWMA with (κ_1, κ_2) and $\kappa_2 > \kappa_1$, where κ_2 is much larger, will reduce ARL_1 and $SDRL_1$ with each change, bringing RMI and RSDI closer to zero and resulting in improved graph performance.

Overall, the evaluation using ARL_1, $SDRL_1$, RMI, and RSDI shows that the double-modified EWMA control chart outperforms both conventional and modified EWMA charts in ARX and ARFIX model settings. This improvement occurs with one-sided and two-sided monitoring. As regards symmetry, the double-modified EWMA chart performs similarly across model structures, control-limit settings, smoothing parameters, and fractional differencing parameters. Thus, the simulation results indicate that the suggested chart detects ARX and ARFIX mean changes effectively and robustly. Note that, in the figure, EWMA denotes the conventional exponentially weighted moving average control chart, MEWMA denotes the modified EWMA control chart, and DMEWMA denotes the double-modified

EWMA control chart. The notation DMEWMA (κ_1, κ_2) represents the double-modified EWMA chart with parameter settings $(\kappa_1, \kappa_2) = (1,1)$, $(1,3)$, $(1,9)$, and $(3,9)$.

5.4. Application to Real Data

In the world's energy markets, WTI and Brent crude oil are two of the most significant benchmarks for crude oil. They are suitable empirical datasets for assessing symmetric control chart theories because their price patterns reflect volatility, uncertainty, and shifting macroeconomic circumstances. The capacity of a monitoring method to provide balanced detection performance for both upward and downward movements is referred to as symmetry in this context. However, because rising oil prices may have significant financial and economic effects, one-sided upward swings are still very important in crude oil markets. The application of a one-sided upper control chart to the crude oil data is justified by the economic importance of detecting sudden increases in crude oil prices. Kilian [34] said oil price increases may be the result of precautionary demand shocks associated with concerns about future oil availability and uncertainty in the global oil market. Aloui [35] and Abuzayed [36] show that the risk of oil prices going up and down affects stock markets, especially when the markets are under a lot of stress. These are elements affecting stock markets. Hence, it is practically important to track the increasing volatility of the crude oil prices, as it has the capacity to operate as an early warning indication of turbulence in the market and risks to the economy.

Monthly WTI and Brent crude oil price data from January 2012 to February 2026 were obtained from Yahoo Finance at https://finance.yahoo.com/ (accessed on 1 March 2026), yielding 170 monthly observations. For the empirical applications, two datasets are considered. The first uses WTI crude oil prices, measured in USD, as the response variable, with the US Dollar Index and the Volatility Index as exogenous variables. The second uses Brent crude oil prices, measured in USD, as the response variable, with WTI crude oil prices and the US 10-year treasury yield as exogenous variables. The ARX$(1,2)$ and ARFIX$(1, 0.14, 2)$ models are fitted to the WTI and Brent crude oil datasets, respectively, to model their dependence structures. The latter generalizes this structure by including the fractional differencing parameter $d = 0.14$ to capture the long-memory behavior, while the former contains one autoregressive term and two exogenous variables. The fitted ARX$(1,2)$ model for WTI crude oil prices and the fitted ARFIX$(1, 0.14, 2)$ model for Brent crude oil prices with statistically significant coefficients at the 0.05 level are shown in Table 2. The RMSE and MAPE values of the fitted ARX$(1,2)$ model are 6.0127 and 7.5320%, respectively. The RMSE and MAPE for the fitted ARFIX$(1, 0.14, 2)$ model for the Brent dataset are 4.6834 and 16.3299%, respectively. The p-values from the Ljung–Box and the Kolmogorov–Smirnov tests are greater than 0.05 for both models, indicating that there is no significant autocorrelation in the residuals, and they are compatible with the assumed exponential white noise distribution.

For the WTI crude oil dataset, the fitted ARX$(1,2)$ model is expressed as

$$y_t = 0.9649 y_{t-1} + 0.0596 x_{1,t} - 0.1990 x_{2,t} + \varepsilon_t, \qquad \varepsilon_t \sim \text{Exp}(4.6764),$$

where y_t denotes the WTI crude oil price, $x_{1,t}$ represents the US Dollar Index, $x_{2,t}$ represents the Volatility Index, and ε_t is the exponential white noise error term.

The fitted ARFIX$(1, 0.14, 2)$ model for the Brent crude oil dataset is expressed as

$$(1 - 0.5156B)(1 - B)^{0.14} y_t = 0.3416 x_{1,t} - 1.3053 x_{2,t} + \varepsilon_t, \qquad \varepsilon_t \sim \text{Exp}(3.3817),$$

where y_t denotes the Brent crude oil price, $x_{1,t}$ represents the WTI crude oil price, $x_{2,t}$ represents the US 10-year treasury yield, and B is the backward-shift operator.

Table 2. Estimated coefficients and diagnostic results of the fitted ARX$(1,2)$ and ARFIX$(1,0.14,2)$ models for crude oil prices.

Dataset	Parameter	Estimate	Std. Error	*t*-Value	*p*-Value
WTI–ARX$(1,2)$	WTI AR(1)	0.9649	0.0199	48.453	<0.0001
	$x_{1,t}$	0.0596	0.0208	2.870	0.0041
	$x_{2,t}$	−0.1990	0.0759	−2.623	0.0087
	Ljung–Box p-value	0.6462			
	KS test p-value	0.2290			
	Mean of exponential residuals	4.6764			
Brent–ARFIX$(1,0.14,2)$	Brent AR(1)	0.5156	0.0538	9.581	<0.0001
	$x_{1,t}$	0.3416	0.0371	9.216	<0.0001
	$x_{2,t}$	−1.3053	0.4352	−2.999	0.0027
	Ljung–Box p-value	0.2698			
	KS test p-value	0.4310			
	Mean of exponential residuals	3.3817			

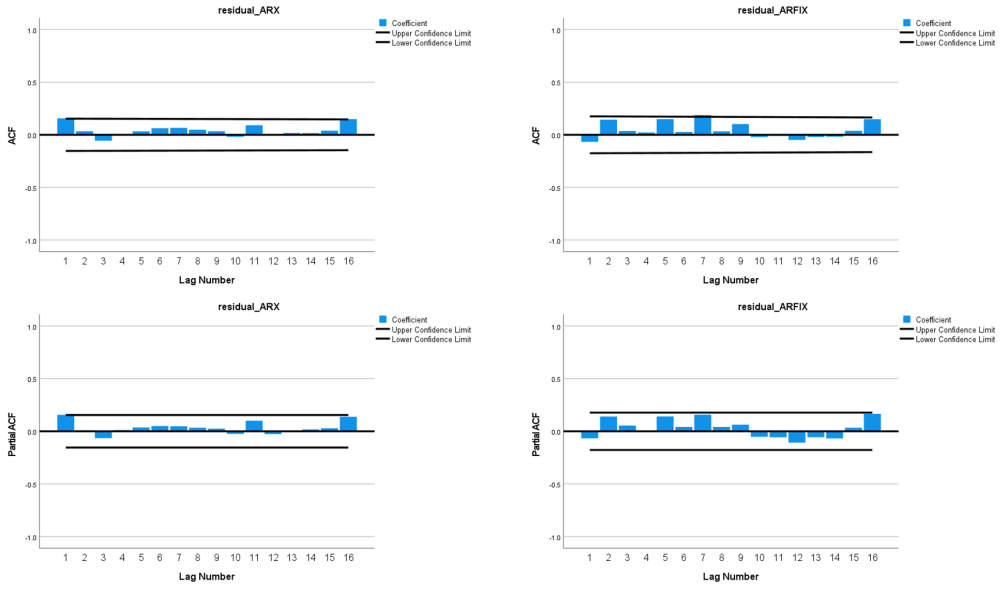
As well, the residual diagnostics of the fitted models are further shown in Figures 1 and 2. The residuals' white noise nature is supported by the ACF, PACF, and residual-time plots, which lack a discernible systematic structure.

The fitted ARX$(1,2)$ and ARFIX$(1,0.14,2)$ models are used to assess the double-modified EWMA, modified EWMA, and standard EWMA control charts on real financial time-series datasets. The study compares one-sided monitoring systems with a set lower control limit of LCL $= 0$. Out-of-control average run length ARL_1, standard deviation of run length SDRL_1, relative mean index (RMI), and relative standard deviation index assess performance. Lower ARL_1 and SDRL_1 values imply increased detection speed and stability, whereas lower RMI and RSDI values suggest improved performance. The double-modified EWMA chart is assessed with four parameter settings: $(\kappa_1,\kappa_2) = (1,1), (1,3), (1,9)$, and $(3,9)$. The selection $(\kappa_1,\kappa_2) = (3,9)$ generally results in the lowest ARL_1 and SDRL_1 values, suggesting better detection of process mean shifts and more consistent run-length behavior. The double-modified EWMA control chart outperforms the standard and modified EWMA charts in the case of real data for all shift magnitudes. The modified EWMA chart is an improvement of the traditional EWMA chart; however, it is not as effective as the double-modified chart, especially in detecting very small shifts in the process mean. The double-modified EWMA chart, particularly with $(\kappa_1,\kappa_2) = (3,9)$, offers the best monitoring performance in one-sided settings with LCL $= 0$, as confirmed by RMI and RSDI findings.

Real-data results match simulation outcomes. The simulation research reveals that the double-modified EWMA chart outperforms the conventional and modified EWMA charts in terms of ARL_1, SDRL_1, RMI, and RSDI. Although real-data applications for WTI and Brent crude oil prices use a one-sided monitoring approach with LCL $= 0$, the same performance trend is seen. This suggests that the suggested chart detects crude oil price upward mean movements quicker .

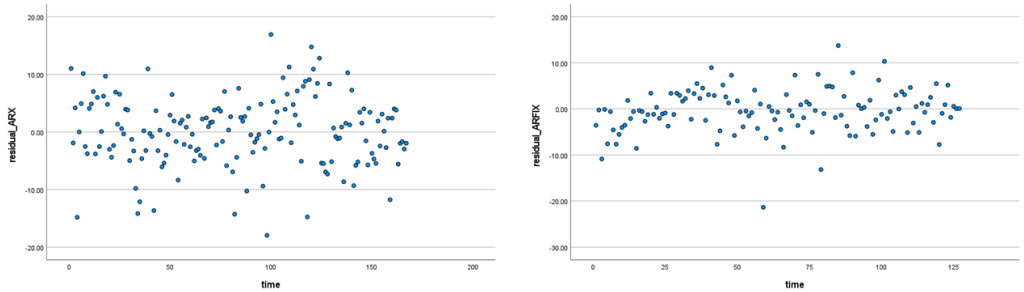
Following the application of the ARX$(1,2)$ and ARFIX$(1,0.14,2)$ models to the actual financial time-series datasets, the EWMA, modified EWMA, and double-modified EWMA control charts are used as previously outlined. After that, all charts are used to assess their efficacy in identifying alterations in the process mean. The smoothing value is set at $\lambda = 0.3$, and the charts are executed as one-sided monitoring schemes with LCL $= 0$. This context is suitable for WTI and Brent crude oil prices, since upward fluctuations are especially significant in energy markets. Significant escalations in crude oil prices may result in elevated production costs, inflationary pressures, and increased financial instability. Therefore, unilateral upward monitoring provides an effective framework for identifying the significant changes and assessing risk in crude oil price dynamics. The

detection performance of the three control charts under the fitted ARX$(1,2)$ model for monthly WTI crude oil prices from January 2012 to February 2026 is presented in Figure A6. The modified EWMA and conventional EWMA charts give signals later at the 13th and 20th observations, respectively. The double-modified EWMA chart detects the first out-of-control signal at the second observation. This reduction in detection delay shows that the double-modified EWMA chart responds more quickly to upward mean shifts in the WTI crude oil price series.



(**a**) The residual diagnostics for ARX(1, 2). (**b**) The residual diagnostics for ARFIX(1, 0.14, 2).

Figure 1. The residual diagnostic plots based on ACF and PACF of the fitted models for two datasets: (**a**) ARX(1, 2) model; and (**b**) ARFIX(1, 0.14, 2) model.



(**a**) Residuals versus time for ARX(1, 2). (**b**) Residuals versus time for ARFIX(1, 0.14, 2).

Figure 2. Residuals versus time for the fitted models based on two datasets: (**a**) residuals versus time for ARX(1, 2); and (**b**) residuals versus time for ARFIX(1, 0.14, 2).

Figure A7 shows the associated results for monthly Brent crude oil prices using the fitted ARFIX$(1, 0.14, 2)$ model. The first out-of-control signal of the double-modified EWMA chart is detected at the second observation, while the modified EWMA and the classical EWMA charts signal at the eighth and 11th observations, respectively. This result verifies the effectiveness of the proposed chart even when fractional differencing is included to model long-memory behavior. Overall, Figures A6 and A7 indicate that the double-modified EWMA control chart detects changes in the upward direction of the process mean earlier and more effectively than the conventional EWMA and the modified EWMA charts. These graphical findings are consistent with the numerical comparison based on

ARL_1, $SDRL_1$, RMI, and RSDI, supporting the practical usefulness of the proposed chart for monitoring WTI and Brent crude oil price processes.

However, in practice, the choice between one-sided and two-sided monitoring plans depends on different applications. A one-sided control chart is suitable when the operator is interested in changes in only one direction, such as an increase in crude oil prices, which may indicate market volatility or economic risk. A two-sided control chart is suitable when both upward and downward changes are significant; for example, you want to detect increases or decreases at the process level. Therefore, the choice between one-sided or two-sided monitoring should depend on the practical objectives of the monitoring problem and the type of process change considered important. In this research focused on crude oil, greater importance is placed on the upper limit (one-sided) chart because the primary practical concern is the early detection of sudden price increases, which justifies the use of a one-sided chart specifically for this purpose.

6. Conclusions

This research formulated and assessed the double-modified EWMA control chart for tracking changes in process mean under ARX(p, r) and ARFIX(p, d, r) models. A definitive closed-form ARL solution was obtained and juxtaposed using the numerical integral equation (NIE) approach. The findings indicated that the ARL values derived from the explicit closed-form solution were markedly consistent with those obtained via the NIE technique, while necessitating much less computational effort. This validates the computational efficacy and precision of the suggested analytical method.

The simulation results showed that the double-modified EWMA control chart performed better than the traditional EWMA and modified EWMA charts for ARL_1, $SDRL_1$, RMI, and RSDI. Lower ARL_1 and $SDRL_1$ values indicated faster and more consistent detection of changes in the process mean, and lower values of RMI and RSDI verified a better overall relative performance. The parameter setting $(\kappa_1, \kappa_2) = (3, 9)$ frequently yielded the most robust detection performance among those evaluated. The proposed graphic was then applied to actual crude oil price data. The WTI crude oil series was modeled by ARX$(1, 2)$ taking the US Dollar Index and the Volatility Index as exogenous factors, while the Brent crude oil series was modeled by ARFIX$(1, 0.14, 2)$ with WTI crude oil prices and the US 10-year treasury yield as exogenous variables. The diagnostic tests confirmed the adequacy of the fitted models. The empirical results are in agreement with the simulation results, and the double-modified EWMA chart is found to be more effective in detecting out-of-control signals as compared to the traditional EWMA and modified EWMA charts. The results obtained in this study agree with the findings of Karoon and Areepong [26] which confirmed that modified EWMA-type control charts are better than the conventional EWMA chart in terms of detection sensitivity and reducing the average run length. The results confirm that the double-modified EWMA control chart is an effective, robust and computationally economical monitoring technique for autoregressive and fractionally integrated autoregressive systems. The real-data applications focus on one-sided upward monitoring with LCL $= 0$, but are consistent with the symmetric monitoring behavior observed in the simulation study.

In addition, the proposed DMEWMA control chart can also be useful for healthcare, industrial, and business sectors, especially when it is critical to detect changes in a process quickly. Businesses can use this chart to ensure quality control and stable production and to identify problems. It is useful to healthcare organizations for tracking infection rates, medical conditions, and quality of service metrics over time. However, the proposed final method does not show satisfactory performance for the present time-series data.

Future research may extend the proposed framework to ARMA, ARIMA, ARFIMA, and multivariate time-series models by including more exogenous variables x_t. These changes would allow the control chart to account for external economic and financial factors and thus enhance the effectiveness of real-time monitoring for complex financial and economic data. The proposed approach can be applied to many types of time-series data, e.g., exchange rates, inflation indices, stock market indices, energy prices, and environmental data, to assess its flexibility and real-world utility. Moreover, future research may further compare the proposed DMEWMA chart with recent adaptive EWMA and mixed memory control charts to provide a broader evaluation of detection performance.

Author Contributions: Conceptualization, K.K. and Y.A.; methodology, K.K.; software, K.K.; validation, S.S. and Y.A.; formal analysis, K.K.; investigation, K.K.; writing—original draft preparation, K.K.; writing—review and editing, K.K., S.S. and Y.A.; visualization, K.K.; supervision, Y.A.; funding acquisition, Y.A. All authors have read and agreed to the published version of the manuscript.

Funding: This research budget was allocated by the National Science, Research, and Innovation Fund (NSRF) and King Mongkut's University of Technology North Bangkok (Project no. KMUTNB-FF-69-B-05).

Data Availability Statement: The dataset can be found at https://finance.yahoo.com/ (accessed on 1 March 2026).

Acknowledgments: The authors are grateful to the editor and referees for their valuable time and effort put into this manuscript.

Conflicts of Interest: The authors declare no conflicts of interest.

Abbreviations

The following abbreviations are used in this manuscript:

EWMA	Exponentially Weighted Moving Average
MEWMA	Modified Exponentially Weighted Moving Average
DEWMA	Double-Modified Exponentially Weighted Moving Average
ARL	Average Run Length
ARL_0	Average Run Length under In-Control Conditions
ARL_1	Average Run Length under Out-of-Control Conditions
SDRL	Standard Deviation of Run Length
$SDRL_0$	Standard Deviation of Run Length under In-Control Conditions
$SDRL_1$	Standard Deviation of Run Length under Out-of-Control Conditions
RMI	Relative Mean Index
RSDI	Relative Standard Deviation Index
ARX	Autoregressive Model with Exogenous Variables
ARFIX	Autoregressive Fractionally Integrated Model with Exogenous Variables
NIE	Numerical Integral Equation

Appendix A

Table A1. Comparative performance of the one-sided EWMA, modified EWMA, and double-modified EWMA control charts with control limits set at $[0, \text{UCL}]$ under the ARX$(1,1)$ model using the explicit closed-form solution based on simulated data with parameters $\vartheta = 1$, and $\phi_1 = 0.1$, when the determined ARL_0 equals 370.

Model	λ	Control Chart	δ	0.001	0.0025	0.005	0.01	0.025	0.1	0.25	0.5	Indices	
ARX(1, 1)	0.05	EWMA	ARL_1	362.014	350.282	331.641	297.526	216.222	50.279	5.340	1.217	RMI	4.344
			SDRL_1	361.514	349.782	331.141	297.026	215.721	49.777	4.814	0.514	RSDI	4.569
		Modified EWMA with $\kappa = 1$	ARL_1	269.740	191.742	129.380	78.383	35.917	9.766	4.164	2.373	RMI	0.803
			SDRL_1	269.240	191.241	128.879	77.881	35.413	9.252	3.630	1.805	RSDI	1.040
		Double-Modified EWMA $\kappa_1 = 1$	ARL_1	263.803	184.382	122.797	73.648	33.527	9.167	3.972	2.304	RMI	0.716
		$\kappa_2 = 1$	SDRL_1	263.303	183.881	122.296	73.146	33.023	8.652	3.436	1.733	RSDI	0.938
		$\kappa_1 = 1$	ARL_1	220.164	137.095	84.352	47.892	21.185	6.115	2.966	1.927	RMI	0.235
		$\kappa_2 = 3$	SDRL_1	219.663	136.594	83.850	47.389	20.679	5.592	2.415	1.337	RSDI	0.371
		$\kappa_1 = 1$	ARL_1	203.579	121.760	73.148	40.939	18.029	5.341	2.702	1.823	RMI	0.100
		$\kappa_2 = 9$	SDRL_1	203.078	121.259	72.647	40.436	17.521	4.815	2.144	1.225	RSDI	0.213
		$\kappa_1 = 3$	ARL_1	197.982	116.898	69.721	38.860	17.099	5.113	2.623	1.792	RMI	0.059
		$\kappa_2 = 9$	SDRL_1	197.481	116.397	69.219	38.356	16.591	4.586	2.063	1.191	RSDI	0.165
	0.10	EWMA	ARL_1	366.207	359.586	348.857	328.498	275.238	122.172	32.457	6.918	RMI	8.273
			SDRL_1	365.707	359.086	348.357	327.998	274.738	121.671	31.953	6.398	RSDI	9.244
		Modified EWMA with $\kappa = 1$	ARL_1	263.064	183.476	121.992	73.067	33.221	9.071	3.928	2.280	RMI	0.618
			SDRL_1	262.564	182.975	121.491	72.565	32.717	8.557	3.392	1.708	RSDI	0.673
		Double-Modified EWMA $\kappa_1 = 1$	ARL_1	253.072	171.594	111.736	65.901	29.687	8.197	3.648	2.179	RMI	0.491
		$\kappa_2 = 1$	SDRL_1	252.572	171.093	111.235	65.399	29.183	7.680	3.108	1.603	RSDI	0.534
		$\kappa_1 = 1$	ARL_1	217.292	134.246	82.202	46.531	20.558	5.959	2.912	1.905	RMI	0.139
		$\kappa_2 = 3$	SDRL_1	216.791	133.745	81.700	46.028	20.052	5.436	2.360	1.313	RSDI	0.152
		$\kappa_1 = 1$	ARL_1	203.221	121.473	72.952	40.822	17.977	5.329	2.698	1.822	RMI	0.032
		$\kappa_2 = 9$	SDRL_1	202.720	120.972	72.450	40.318	17.470	4.803	2.141	1.224	RSDI	0.035
		$\kappa_1 = 3$	ARL_1	198.721	117.518	70.152	39.120	17.216	5.143	2.635	1.797	RMI	0
		$\kappa_2 = 9$	SDRL_1	198.220	117.017	69.650	38.617	16.709	4.616	2.075	1.197	RSDI	0
	0.15	EWMA	ARL_1	365.798	358.907	347.797	326.903	273.353	126.313	39.776	10.955	RMI	8.921
			SDRL_1	365.298	358.407	347.297	326.403	272.853	125.812	39.273	10.443	RSDI	10.124
		Modified EWMA with $\kappa = 1$	ARL_1	257.164	176.146	115.541	68.500	30.938	8.486	3.729	2.201	RMI	0.526
			SDRL_1	256.664	175.645	115.040	67.998	30.433	7.971	3.190	1.626	RSDI	0.572
		Double-Modified EWMA $\kappa_1 = 1$	ARL_1	243.931	161.461	103.367	60.234	26.949	7.512	3.418	2.090	RMI	0.380
		$\kappa_2 = 1$	SDRL_1	243.430	160.960	102.866	59.732	26.444	6.994	2.875	1.510	RSDI	0.413
		$\kappa_1 = 1$	ARL_1	214.958	132.010	80.540	45.488	20.081	5.841	2.871	1.889	RMI	0.114
		$\kappa_2 = 3$	SDRL_1	214.457	131.509	80.038	44.986	19.575	5.318	2.318	1.296	RSDI	0.124
		$\kappa_1 = 1$	ARL_1	203.169	121.409	72.903	40.791	17.964	5.327	2.699	1.823	RMI	0.026
		$\kappa_2 = 9$	SDRL_1	202.668	120.908	72.401	40.288	17.457	4.801	2.141	1.225	RSDI	0.029
		$\kappa_1 = 3$	ARL_1	199.439	118.150	70.599	39.392	17.339	5.175	2.647	1.803	RMI	0
		$\kappa_2 = 9$	SDRL_1	198.938	117.649	70.097	38.889	16.832	4.648	2.088	1.203	RSDI	0

Note: The subscript 1 in ARL_1 and SDRL_1 denotes the out-of-control average run length. UCL values are set as follows: $\lambda = 0.05$: $H_0 = 0.000000012661$ for EWMA, $H_1 = 0.3339875$ for modified EWMA, and $H = 0.3691633, 1.10594, 3.316192$, and 9.377654 for double-modified EWMA with (κ_1, κ_2) equals $(1,1), (1,3), (1,9), (3,9)$. $\lambda = 0.1$: $H_0 = 0.0005357$ for EWMA, $H_1 = 0.3376846$ for modified EWMA, and $H = 0.411796, 1.221693, 3.653111$, and 9.79979 for double-modified EWMA with (κ_1, κ_2) equals $(1,1), (1,3), (1,9), (3,9)$. $\lambda = 0.2$: $H_0 = 0.010494$ for EWMA, $H_1 = 0.341825$ for modified EWMA, and $H = 0.4586384, 1.342759, 3.999171$, and 10.232783 for double-modified EWMA with (κ_1, κ_2) equals $(1,1), (1,3), (1,9), (3,9)$.

Table A2. Comparative performance of the one-sided EWMA, modified EWMA, and double-modified EWMA control charts with control limits set at $[0, \text{UCL}]$ under the ARX$(2,1)$ model using the explicit closed-form solution based on simulated data with parameters $\vartheta = 1$, $\phi_1 = 0.1$, and $\phi_2 = 0.4$ when the determined ARL_0 equals 370.

Model	λ	Control Chart		δ	0.001	0.0025	0.005	0.01	0.025	0.1	0.25	0.5	Indices	
ARX(2, 1)	0.05	EWMA		ARL_1	362.086	350.142	331.181	296.530	214.260	48.548	5.009	1.190	RMI	4.860
				SDRL_1	361.586	349.642	330.681	296.030	213.759	48.045	4.481	0.476	RSDI	5.143
		Modified EWMA		ARL_1	260.352	180.184	119.056	70.909	32.020	8.611	3.675	2.123	RMI	0.793
		with $\kappa = 1$		SDRL_1	259.852	179.683	118.555	70.407	31.516	8.096	3.135	1.544	RSDI	1.023
		Double-Modified EWMA	$\kappa_1 = 1$	ARL_1	254.221	172.889	112.773	66.532	29.872	8.089	3.512	2.066	RMI	0.706
			$\kappa_2 = 1$	SDRL_1	253.721	172.388	112.272	66.030	29.368	7.573	2.970	1.484	RSDI	0.920
			$\kappa_1 = 1$	ARL_1	208.831	126.440	76.457	42.905	18.829	5.431	2.660	1.757	RMI	0.223
			$\kappa_2 = 3$	SDRL_1	208.330	125.939	75.956	42.402	18.322	4.906	2.101	1.153	RSDI	0.352
			$\kappa_1 = 1$	ARL_1	191.908	111.687	66.050	36.598	16.020	4.758	2.436	1.672	RMI	0.088
			$\kappa_2 = 9$	SDRL_1	191.407	111.186	65.548	36.095	15.512	4.229	1.870	1.060	RSDI	0.194
			$\kappa_1 = 3$	ARL_1	186.393	107.093	62.898	34.723	15.195	4.560	2.369	1.646	RMI	0.048
			$\kappa_2 = 9$	SDRL_1	185.892	106.592	62.396	34.220	14.687	4.030	1.801	1.031	RSDI	0.146
	0.10	EWMA		ARL_1	365.857	359.018	347.946	326.968	272.313	117.633	29.966	6.166	RMI	9.018
				SDRL_1	365.357	358.518	347.446	326.468	271.813	117.132	29.462	5.644	RSDI	10.195
		Modified EWMA		ARL_1	253.231	171.775	111.834	65.880	29.543	7.992	3.470	2.044	RMI	0.626
		with $\kappa = 1$		SDRL_1	252.731	171.274	111.333	65.378	29.038	7.476	2.928	1.461	RSDI	0.687
		Double-Modified EWMA	$\kappa_1 = 1$	ARL_1	242.538	159.880	102.019	59.254	26.368	7.230	3.233	1.962	RMI	0.496
			$\kappa_2 = 1$	SDRL_1	242.037	159.379	101.518	58.752	25.863	6.711	2.686	1.374	RSDI	0.544
			$\kappa_1 = 1$	ARL_1	205.345	123.329	74.227	41.538	18.214	5.282	2.609	1.737	RMI	0.140
			$\kappa_2 = 3$	SDRL_1	204.844	122.828	73.726	41.035	17.707	4.756	2.049	1.132	RSDI	0.154
			$\kappa_1 = 1$	ARL_1	191.282	111.153	65.679	36.377	15.923	4.735	2.428	1.669	RMI	0.032
			$\kappa_2 = 9$	SDRL_1	190.781	110.652	65.177	35.873	15.415	4.206	1.862	1.057	RSDI	0.036
			$\kappa_1 = 3$	ARL_1	186.728	107.375	63.093	34.840	15.247	4.574	2.374	1.649	RMI	0
			$\kappa_2 = 9$	SDRL_1	186.227	106.874	62.591	34.336	14.739	4.043	1.806	1.034	RSDI	0
	0.15	EWMA		ARL_1	365.912	358.543	346.694	324.513	268.283	118.980	35.736	9.479	RMI	9.533
				SDRL_1	365.412	358.043	346.194	324.013	267.783	118.479	35.233	8.965	RSDI	10.951
		Modified EWMA		ARL_1	246.667	164.220	105.500	61.557	27.446	7.471	3.298	1.978	RMI	0.535
		with $\kappa = 1$		SDRL_1	246.166	163.719	104.999	61.055	26.941	6.954	2.753	1.391	RSDI	0.586
		Double-Modified EWMA	$\kappa_1 = 1$	ARL_1	232.907	149.729	93.950	53.950	23.869	6.621	3.034	1.887	RMI	0.385
			$\kappa_2 = 1$	SDRL_1	232.406	149.228	93.449	53.447	23.364	6.101	2.484	1.294	RSDI	0.422
			$\kappa_1 = 1$	ARL_1	202.695	120.917	72.494	40.476	17.737	5.166	2.570	1.722	RMI	0.115
			$\kappa_2 = 3$	SDRL_1	202.194	120.416	71.992	39.973	17.230	4.639	2.008	1.115	RSDI	0.126
			$\kappa_1 = 1$	ARL_1	190.874	110.798	65.432	36.228	15.857	4.720	2.423	1.667	RMI	0.027
			$\kappa_2 = 9$	SDRL_1	190.373	110.297	64.930	35.725	15.349	4.190	1.857	1.055	RSDI	0.029
			$\kappa_1 = 3$	ARL_1	187.088	107.679	63.302	34.964	15.303	4.588	2.380	1.651	RMI	0
			$\kappa_2 = 9$	SDRL_1	186.587	107.178	62.800	34.461	14.794	4.057	1.812	1.037	RSDI	0

Note: UCL values are set as follows: $\lambda = 0.05$: $H_0 = 0.000000008492$ for EWMA, $H_1 = 0.3339875$ for modified EWMA, and $H = 0.246741, 0.7392, 2.2165$, and 6.26791 for double-modified EWMA with (κ_1, κ_2) equals $(1,1), (1,3), (1,9), (3,9)$. $\lambda = 0.1$: $H_0 = 0.0003586$ for EWMA, $H_1 = 0.2251535$ for modified EWMA, and $H = 0.2745512, 0.8143531, 2.434894$, and 6.531635 for double-modified EWMA with (κ_1, κ_2) equals $(1,1), (1,3), (1,9), (3,9)$. $\lambda = 0.2$: $H_0 = 0.006996$ for EWMA, $H_1 = 0.227392$ for modified EWMA, and $H = 0.3050355, 0.892617, 2.657996$, and 6.800651 for double-modified EWMA with (κ_1, κ_2) equals $(1,1), (1,3), (1,9), (3,9)$.

Table A3. Comparative performance of the two-sided EWMA, modified EWMA, and double-modified EWMA control charts with control limits set at [LCL, UCL] under the ARX(2, 2) model using the explicit closed-form solution based on simulated data with parameters $\vartheta = 0$, $\phi_1 = \phi_2 = 0.2$, when the determined ARL_0 equals 370.

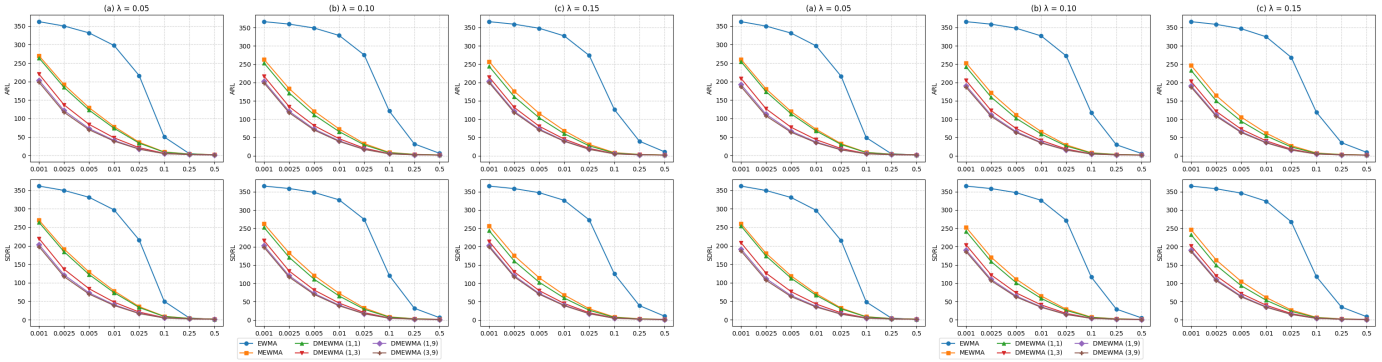
Model	λ	Control Chart		δ	0.001	0.0025	0.005	0.01	0.025	0.1	0.25	0.5	Indices	
ARX(2, 2)	0.05	EWMA		ARL_1	364.789	357.035	344.524	320.971	260.606	100.137	21.206	3.819	RMI	7.654
				$SDRL_1$	364.289	356.535	344.024	320.471	260.106	99.636	20.700	3.281	RSDI	8.479
		Modified EWMA		ARL_1	234.284	151.009	94.934	54.606	24.214	6.756	3.112	1.938	RMI	0.393
		with $\kappa = 1$		$SDRL_1$	233.783	150.508	94.433	54.103	23.709	6.236	2.564	1.348	RSDI	0.431
		Double-Modified EWMA	$\kappa_1 = 1$	ARL_1	229.868	146.641	91.572	52.441	23.209	6.513	3.033	1.909	RMI	0.350
			$\kappa_2 = 1$	$SDRL_1$	229.367	146.140	91.071	51.939	22.703	5.992	2.483	1.318	RSDI	0.384
			$\kappa_1 = 1$	ARL_1	201.412	119.856	71.769	40.057	17.574	5.155	2.585	1.740	RMI	0.100
			$\kappa_2 = 3$	$SDRL_1$	200.911	119.355	71.267	39.553	17.066	4.628	2.024	1.135	RSDI	0.109
			$\kappa_1 = 1$	ARL_1	191.325	111.179	65.704	36.403	15.952	4.764	2.453	1.689	RMI	0.024
			$\kappa_2 = 9$	$SDRL_1$	190.824	110.678	65.202	35.900	15.444	4.234	1.888	1.079	RSDI	0.026
			$\kappa_1 = 3$	ARL_1	187.997	108.410	63.805	35.273	15.453	4.643	2.412	1.673	RMI	0
			$\kappa_2 = 9$	$SDRL_1$	187.496	107.909	63.303	34.769	14.945	4.113	1.846	1.061	RSDI	0
	0.10	EWMA		ARL_1	365.859	358.577	346.872	324.977	269.558	122.323	38.648	10.913	RMI	9.732
				$SDRL_1$	365.359	358.077	346.372	324.477	269.058	121.822	38.145	10.401	RSDI	11.209
		Modified EWMA		ARL_1	229.537	146.309	91.314	52.271	23.124	6.486	3.019	1.901	RMI	0.340
		with $\kappa = 1$		$SDRL_1$	229.036	145.808	90.813	51.769	22.619	5.965	2.469	1.309	RSDI	0.372
		Double-Modified EWMA	$\kappa_1 = 1$	ARL_1	222.639	139.466	86.092	48.937	21.587	6.117	2.900	1.858	RMI	0.274
			$\kappa_2 = 1$	$SDRL_1$	222.138	138.965	85.590	48.434	21.081	5.594	2.348	1.262	RSDI	0.300
			$\kappa_1 = 1$	ARL_1	199.948	118.435	70.733	39.418	17.286	5.084	2.561	1.731	RMI	0.082
			$\kappa_2 = 3$	$SDRL_1$	199.447	117.934	70.231	38.914	16.778	4.557	1.999	1.125	RSDI	0.090
			$\kappa_1 = 1$	ARL_1	191.284	111.143	65.679	36.388	15.946	4.763	2.453	1.690	RMI	0.019
			$\kappa_2 = 9$	$SDRL_1$	190.783	110.642	65.177	35.885	15.438	4.234	1.888	1.080	RSDI	0.021
			$\kappa_1 = 3$	ARL_1	188.670	108.907	64.131	35.463	15.537	4.665	2.420	1.677	RMI	0
			$\kappa_2 = 9$	$SDRL_1$	188.169	108.406	63.629	34.960	15.029	4.135	1.854	1.065	RSDI	0
	0.15	EWMA		ARL_1	354.244	332.458	301.145	252.331	165.907	50.942	15.481	5.357	RMI	4.964
				$SDRL_1$	353.744	331.958	300.645	251.831	165.406	50.439	14.973	4.832	RSDI	5.553
		Modified EWMA		ARL_1	225.533	142.236	88.171	50.248	22.183	6.252	2.939	1.869	RMI	0.293
		with $\kappa = 1$		$SDRL_1$	225.032	141.735	87.669	49.746	21.677	5.731	2.388	1.274	RSDI	0.321
		Double-Modified EWMA	$\kappa_1 = 1$	ARL_1	217.138	134.032	81.991	46.341	20.395	5.826	2.802	1.819	RMI	0.216
			$\kappa_2 = 1$	$SDRL_1$	216.637	133.531	81.489	45.838	19.889	5.302	2.247	1.221	RSDI	0.236
			$\kappa_1 = 1$	ARL_1	198.386	117.204	69.896	38.920	17.067	5.032	2.543	1.724	RMI	0.067
			$\kappa_2 = 3$	$SDRL_1$	197.885	116.703	69.394	38.417	16.559	4.504	1.981	1.117	RSDI	0.073
			$\kappa_1 = 1$	ARL_1	191.323	111.198	65.722	36.416	15.959	4.767	2.455	1.691	RMI	0.016
			$\kappa_2 = 9$	$SDRL_1$	190.822	110.697	65.220	35.913	15.451	4.238	1.890	1.081	RSDI	0.017
			$\kappa_1 = 3$	ARL_1	189.232	109.378	64.455	35.657	15.623	4.687	2.428	1.681	RMI	0
			$\kappa_2 = 9$	$SDRL_1$	188.731	108.877	63.953	35.153	15.115	4.157	1.863	1.070	RSDI	0

Note: LCL equal to 0.4, and UCL values are set as follows: $\lambda = 0.05$: $H_0 = 0.400027852$ for EWMA, $H_1 = 0.652098$ for modified EWMA, and $H = 0.6780877, 1.2226471, 2.856333$, and 7.3366 for double-modified EWMA with (κ_1, κ_2) equals $(1,1), (1,3), (1,9), (3,9)$. $\lambda = 0.1$: $H_0 = 0.408624$ for EWMA, $H_1 = 0.6588586$ for modified EWMA, and $H =$ $0.7136012, 1.311207, 3.104482$, and 7.63767 for double-modified EWMA with (κ_1, κ_2) equals $(1,1), (1,3), (1,9), (3,9)$. $\lambda = 0.2$: $H_0 = 0.41903$ for EWMA, $H_1 = 0.665793$ for modified EWMA, and $H = 0.752077, 1.4033463, 3.358252$, and 7.94512 for double-modified EWMA with (κ_1, κ_2) equals $(1,1), (1,3), (1,9), (3,9)$.

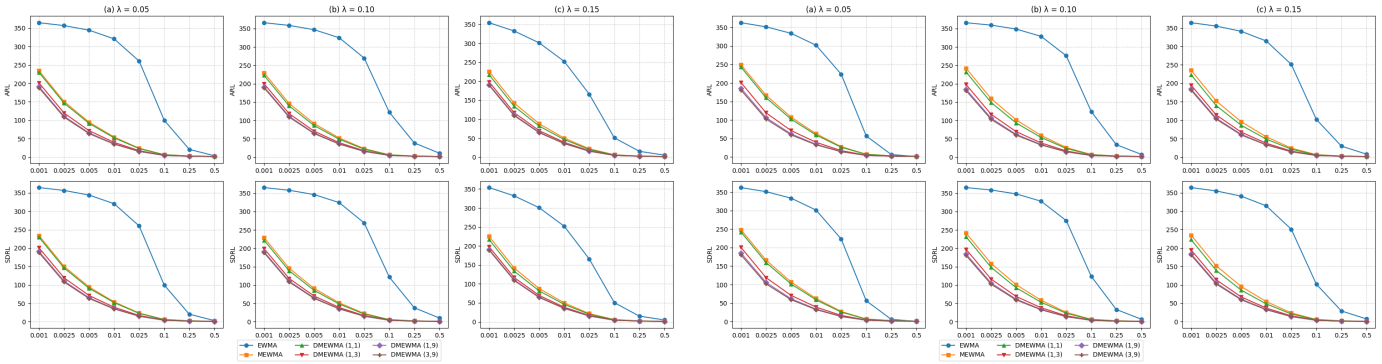
Table A4. Comparative performance of the two-sided EWMA, modified EWMA, and double-modified EWMA control charts with control limits set at [LCL, UCL] under the ARX(3, 2) model using the explicit closed-form solution based on simulated data with parameters $\vartheta = 0$, $\phi_1 = \phi_2 = 0.2$, and $\phi_3 = 0.3$ when the determined ARL_0 equals 370.

Model	λ	Control Chart		δ	0.001	0.0025	0.005	0.01	0.025	0.1	0.25	0.5	Indices	
ARX(3, 2)	0.05	EWMA		ARL_1	362.714	351.693	334.131	301.827	223.817	56.998	6.745	1.346	RMI	5.628
				$SDRL_1$	362.214	351.193	333.631	301.327	223.316	56.495	6.225	0.683	RSDI	6.022
		Modified EWMA		ARL_1	248.741	166.725	107.606	62.971	28.093	7.584	3.304	1.962	RMI	0.670
		with $\kappa = 1$		$SDRL_1$	248.240	166.224	107.105	62.469	27.588	7.066	2.759	1.374	RSDI	0.782
		Double-Modified EWMA	$\kappa_1 = 1$	ARL_1	242.867	160.203	102.251	59.374	26.377	7.174	3.177	1.918	RMI	0.595
			$\kappa_2 = 1$	$SDRL_1$	242.366	159.702	101.750	58.872	25.872	6.655	2.630	1.327	RSDI	0.698
			$\kappa_1 = 1$	ARL_1	201.065	119.411	71.393	39.777	17.389	5.040	2.498	1.675	RMI	0.177
			$\kappa_2 = 3$	$SDRL_1$	200.564	118.910	70.891	39.274	16.882	4.512	1.934	1.063	RSDI	0.226
			$\kappa_1 = 1$	ARL_1	185.702	106.488	62.462	34.439	15.037	4.482	2.315	1.606	RMI	0.058
			$\kappa_2 = 9$	$SDRL_1$	185.201	105.987	61.960	33.935	14.529	3.951	1.744	0.986	RSDI	0.092
			$\kappa_1 = 3$	ARL_1	180.655	102.438	59.736	32.837	14.339	4.317	2.260	1.585	RMI	0.022
			$\kappa_2 = 9$	$SDRL_1$	180.154	101.937	59.234	32.333	13.830	3.784	1.687	0.963	RSDI	0.051
	0.10	EWMA		ARL_1	365.905	359.364	348.765	328.647	275.983	124.072	33.852	7.443	RMI	10.108
				$SDRL_1$	365.405	358.864	348.265	328.147	275.483	123.571	33.349	6.925	RSDI	11.610
		Modified EWMA		ARL_1	241.952	159.221	101.455	58.839	26.114	7.098	3.144	1.902	RMI	0.552
		with $\kappa = 1$		$SDRL_1$	241.451	158.720	100.954	58.336	25.609	6.579	2.597	1.310	RSDI	0.608
		Double-Modified EWMA	$\kappa_1 = 1$	ARL_1	231.857	148.664	93.104	53.373	23.557	6.493	2.957	1.837	RMI	0.439
			$\kappa_2 = 1$	$SDRL_1$	231.356	148.163	92.603	52.870	23.052	5.972	2.406	1.240	RSDI	0.484
			$\kappa_1 = 1$	ARL_1	197.731	116.610	69.445	38.606	16.870	4.915	2.456	1.658	RMI	0.125
			$\kappa_2 = 3$	$SDRL_1$	197.230	116.109	68.943	38.102	16.362	4.387	1.891	1.045	RSDI	0.138
			$\kappa_1 = 1$	ARL_1	184.993	105.947	62.103	34.229	14.946	4.461	2.308	1.603	RMI	0.029
			$\kappa_2 = 9$	$SDRL_1$	184.492	105.446	61.601	33.726	14.438	3.929	1.737	0.983	RSDI	0.032
			$\kappa_1 = 3$	ARL_1	180.892	102.637	59.872	32.917	14.374	4.326	2.263	1.587	RMI	0
			$\kappa_2 = 9$	$SDRL_1$	180.391	102.136	59.370	32.413	13.865	3.793	1.691	0.965	RSDI	0
	0.15	EWMA		ARL_1	364.435	355.425	341.109	314.866	251.448	102.387	29.871	8.183	RMI	9.009
				$SDRL_1$	363.935	354.925	340.609	314.366	250.948	101.886	29.366	7.666	RSDI	10.371
		Modified EWMA		ARL_1	235.451	152.390	96.021	55.261	24.426	6.686	3.009	1.850	RMI	0.473
		with $\kappa = 1$		$SDRL_1$	234.950	151.889	95.519	54.759	23.920	6.165	2.458	1.254	RSDI	0.520
		Double-Modified EWMA	$\kappa_1 = 1$	ARL_1	223.201	139.833	86.287	48.991	21.530	6.005	2.799	1.778	RMI	0.343
			$\kappa_2 = 1$	$SDRL_1$	222.700	139.332	85.786	48.489	21.024	5.483	2.244	1.176	RSDI	0.377
			$\kappa_1 = 1$	ARL_1	195.171	114.424	67.921	37.689	16.464	4.818	2.423	1.646	RMI	0.103
			$\kappa_2 = 3$	$SDRL_1$	194.670	113.923	67.419	37.186	15.956	4.289	1.857	1.031	RSDI	0.113
			$\kappa_1 = 1$	ARL_1	184.608	105.602	61.863	34.086	14.883	4.446	2.303	1.602	RMI	0.024
			$\kappa_2 = 9$	$SDRL_1$	184.107	105.101	61.361	33.582	14.375	3.914	1.732	0.982	RSDI	0.026
			$\kappa_1 = 3$	ARL_1	181.299	102.901	60.036	33.010	14.414	4.336	2.267	1.588	RMI	0
			$\kappa_2 = 9$	$SDRL_1$	180.798	102.400	59.534	32.506	13.905	3.803	1.694	0.967	RSDI	0

Note: LCL equal to 0.1, and UCL values are set as follows: $\lambda = 0.05$: $H_0 = 0.10000005137$ for EWMA, $H_1 = 0.2835405$ for modified EWMA, and $H = 0.3027685, 0.705528, 1.913757$, and 5.227243 for double-modified EWMA with (κ_1, κ_2) equals $(1,1), (1,3), (1,9), (3,9)$. $\lambda = 0.1$: $H_0 = 0.1007513$ for EWMA, $H_1 = 0.2857581$ for modified EWMA, and $H = 0.3261347, 0.7672292, 2.091264$, and 5.438377 for double-modified EWMA with (κ_1, κ_2) equals $(1,1), (1,3), (1,9), (3,9)$. $\lambda = 0.2$: $H_0 = 0.107799$ for EWMA, $H_1 = 0.2881924$ for modified EWMA, and $H = 0.351636, 0.8313504, 2.272247$, and 5.65335 for double-modified EWMA with (κ_1, κ_2) equals $(1,1), (1,3), (1,9), (3,9)$.

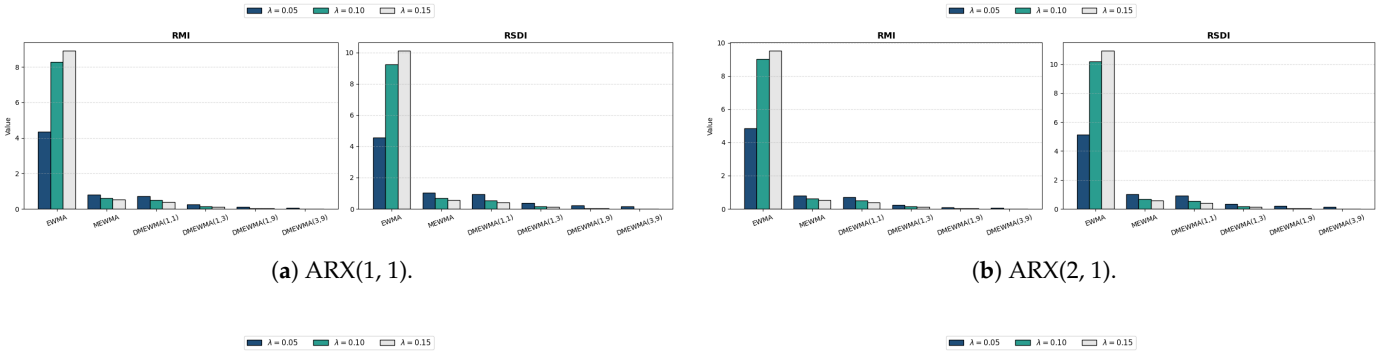


(**a**) ARX(1, 1). (**b**) ARX(2, 1).

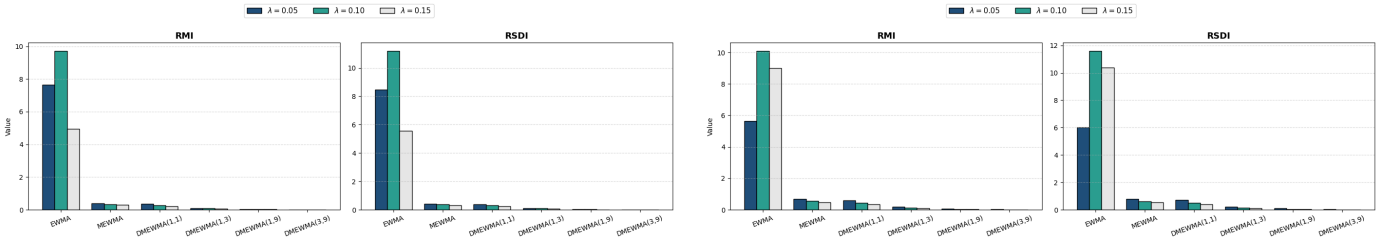


(**c**) ARX(2, 2). (**d**) ARX(3, 2).

Figure A1. The ARL_1 and $SDRL_1$ values vary with the magnitude of the shift (δ), from small-to-moderate levels, under $\lambda = 0.05, 0.1$, and 0.2, for the EWMA, modified EWMA, and double-modified EWMA control charts (with $(\kappa_1, \kappa_2) = (1,1), (1,3), (1,9)$, and $(3,9)$) operating under the ARX(p,r) model: (**a**) ARX$(1,1)$, (**b**) ARX$(2,1)$, (**c**) ARX$(2,2)$, and (**d**) ARX$(3,2)$.



(**a**) ARX(1, 1). (**b**) ARX(2, 1).



(**c**) ARX(2, 2). (**d**) ARX(3, 2).

Figure A2. The RMI and RSDI values under $\lambda = 0.05, 0.1$, and 0.2, for the EWMA, modified EWMA, and double-modified EWMA control charts (with $(\kappa_1, \kappa_2) = (1,1), (1,3), (1,9)$, and $(3,9)$) operating under the ARFIX(p,d,r) model: (**a**) ARX$(1,1)$, (**b**) ARX$(2,1)$, (**c**) ARX$(2,2)$, and (**d**) ARX$(3,2)$.

Table A5. Comparative performance of the one-sided EWMA, modified EWMA, and double-modified EWMA control charts with control limits set at $[0, \text{UCL}]$ under the ARFIX$(1, 0.25, 1)$ model using the explicit closed-form solution based on simulated data with parameters $\vartheta = 0.9$, and $\phi_1 = 0.2$ when the determined ARL_0 equals 370.

Model	λ	Control Chart		δ	0.001	0.0025	0.005	0.01	0.025	0.1	0.25	0.5	Indices	
ARFIX(1, 0.25, 1)	0.05	EWMA		ARL_1	361.929	349.997	331.051	296.430	214.221	48.573	5.015	1.191	RMI	4.843
				SDRL_1	361.429	349.497	330.551	295.930	213.720	48.071	4.488	0.476	RSDI	5.124
		Modified EWMA		ARL_1	260.695	180.527	119.336	71.101	32.116	8.639	3.687	2.129	RMI	0.793
		with $\kappa = 1$		SDRL_1	260.195	180.026	118.835	70.600	31.612	8.124	3.147	1.550	RSDI	1.023
		Double-Modified EWMA	$\kappa_1 = 1$	ARL_1	254.502	173.197	113.030	66.710	29.962	8.115	3.523	2.072	RMI	0.706
			$\kappa_2 = 1$	SDRL_1	254.002	172.696	112.529	66.208	29.457	7.599	2.981	1.490	RSDI	0.920
			$\kappa_1 = 1$	ARL_1	209.180	126.728	76.660	43.030	18.886	5.448	2.667	1.761	RMI	0.223
			$\kappa_2 = 3$	SDRL_1	208.679	126.227	76.159	42.527	18.380	4.922	2.108	1.158	RSDI	0.352
			$\kappa_1 = 1$	ARL_1	192.276	111.963	66.233	36.707	16.070	4.772	2.442	1.676	RMI	0.089
			$\kappa_2 = 9$	SDRL_1	191.775	111.462	65.731	36.203	15.561	4.243	1.877	1.064	RSDI	0.194
			$\kappa_1 = 3$	ARL_1	186.849	107.390	63.085	34.829	15.242	4.574	2.375	1.650	RMI	0.048
			$\kappa_2 = 9$	SDRL_1	186.348	106.889	62.583	34.325	14.734	4.043	1.807	1.035	RSDI	0.147
	0.10	EWMA		ARL_1	365.479	358.653	347.602	326.663	272.103	117.630	30.000	6.179	RMI	8.988
				SDRL_1	364.979	358.153	347.102	326.163	271.603	117.129	29.496	5.657	RSDI	10.158
		Modified EWMA		ARL_1	253.443	172.053	112.079	66.054	29.632	8.018	3.481	2.050	RMI	0.626
		with $\kappa = 1$		SDRL_1	252.943	171.552	111.578	65.552	29.127	7.502	2.939	1.467	RSDI	0.687
		Double-Modified EWMA	$\kappa_1 = 1$	ARL_1	242.749	160.150	102.249	59.413	26.448	7.253	3.242	1.967	RMI	0.496
			$\kappa_2 = 1$	SDRL_1	242.248	159.649	101.748	58.911	25.943	6.734	2.697	1.379	RSDI	0.544
			$\kappa_1 = 1$	ARL_1	205.775	123.647	74.440	41.665	18.272	5.298	2.616	1.741	RMI	0.140
			$\kappa_2 = 3$	SDRL_1	205.274	123.146	73.938	41.162	17.765	4.772	2.056	1.136	RSDI	0.154
			$\kappa_1 = 1$	ARL_1	191.721	111.455	65.874	36.489	15.973	4.749	2.435	1.673	RMI	0.033
			$\kappa_2 = 9$	SDRL_1	191.220	110.954	65.372	35.986	15.465	4.220	1.869	1.061	RSDI	0.036
			$\kappa_1 = 3$	ARL_1	187.021	107.623	63.264	34.943	15.294	4.587	2.380	1.652	RMI	0
			$\kappa_2 = 9$	SDRL_1	186.520	107.122	62.762	34.439	14.786	4.057	1.813	1.038	RSDI	0
	0.15	EWMA		ARL_1	365.970	358.613	346.781	324.629	268.459	119.184	35.841	9.516	RMI	9.519
				SDRL_1	365.470	358.113	346.281	324.129	267.959	118.683	35.338	9.002	RSDI	10.931
		Modified EWMA		ARL_1	246.943	164.524	105.750	61.727	27.530	7.496	3.308	1.983	RMI	0.534
		with $\kappa = 1$		SDRL_1	246.442	164.023	105.249	61.225	27.026	6.978	2.763	1.396	RSDI	0.585
		Double-Modified EWMA	$\kappa_1 = 1$	ARL_1	233.153	150.008	94.177	54.101	23.943	6.642	3.043	1.892	RMI	0.385
			$\kappa_2 = 1$	SDRL_1	232.652	149.507	93.675	53.598	23.437	6.122	2.493	1.299	RSDI	0.422
			$\kappa_1 = 1$	ARL_1	202.915	121.160	72.679	40.594	17.793	5.182	2.577	1.726	RMI	0.114
			$\kappa_2 = 3$	SDRL_1	202.414	120.659	72.177	40.091	17.286	4.655	2.016	1.119	RSDI	0.125
			$\kappa_1 = 1$	ARL_1	191.173	111.056	65.613	36.338	15.908	4.734	2.430	1.671	RMI	0.026
			$\kappa_2 = 9$	SDRL_1	190.672	110.555	65.111	35.835	15.400	4.205	1.864	1.059	RSDI	0.029
			$\kappa_1 = 3$	ARL_1	187.416	107.943	63.481	35.072	15.352	4.602	2.386	1.655	RMI	0
			$\kappa_2 = 9$	SDRL_1	186.915	107.442	62.979	34.568	14.843	4.071	1.818	1.041	RSDI	0

Note: UCL values are set as follows: $\lambda = 0.05$: $H_0' = 0.00000000858$ for EWMA, $H_1' = 0.2256562$ for modified EWMA, and $H' = 0.249425, 0.747241, 2.240612$, and 6.33611 for double-modified EWMA with (κ_1, κ_2) equals $(1,1), (1,3), (1,9), (3,9)$. $\lambda = 0.1$: $H_0' = 0.00036212$ for EWMA, $H_1' = 0.2276142$ for modified EWMA, and $H' = 0.277552, 0.823262, 2.461536$, and 6.60308 for double-modified EWMA with (κ_1, κ_2) equals $(1,1), (1,3), (1,9), (3,9)$. $\lambda = 0.2$: $H_0' = 0.007073$ for EWMA, $H_1' = 0.229889$ for modified EWMA, and $H' = 0.3083861, 0.9024301, 2.687234$, and 6.875473 for double-modified EWMA with (κ_1, κ_2) equals $(1,1), (1,3), (1,9), (3,9)$.

Table A6. Comparative performance of the one-sided EWMA, modified EWMA, and double-modified EWMA control charts with control limits set at $[0, \text{UCL}]$ under the ARFIX$(1, 0.45, 1)$ model using the explicit closed-form solution based on simulated data with parameters $\vartheta = 0.9$, and $\phi_1 = 0.2$ when the determined ARL_0 equals 370.

Model	λ	Control Chart		δ	0.001	0.0025	0.005	0.01	0.025	0.1	0.25	0.5	Indices	
ARFIX(1, 0.45, 1)	0.05	EWMA		ARL_1	362.246	350.202	331.086	296.179	213.441	47.791	4.867	1.179	RMI	5.097
				SDRL_1	361.746	349.702	330.586	295.679	212.940	47.288	4.338	0.459	RSDI	5.409
		Modified EWMA		ARL_1	256.275	175.275	114.778	67.878	30.468	8.159	3.486	2.027	RMI	0.790
		with $\kappa = 1$		SDRL_1	255.775	174.774	114.277	67.376	29.964	7.643	2.943	1.443	RSDI	1.017
		Double-Modified EWMA	$\kappa_1 = 1$	ARL_1	249.861	167.929	108.592	63.638	28.416	7.667	3.334	1.975	RMI	0.702
			$\kappa_2 = 1$	SDRL_1	249.360	167.428	108.091	63.136	27.912	7.149	2.789	1.388	RSDI	0.913
			$\kappa_1 = 1$	ARL_1	203.887	121.984	73.240	40.908	17.897	5.164	2.541	1.692	RMI	0.218
			$\kappa_2 = 3$	SDRL_1	203.386	121.483	72.738	40.405	17.390	4.637	1.979	1.083	RSDI	0.345
			$\kappa_1 = 1$	ARL_1	186.955	107.539	63.183	34.869	15.229	4.531	2.333	1.614	RMI	0.084
			$\kappa_2 = 9$	SDRL_1	186.454	107.038	62.681	34.365	14.720	4.000	1.764	0.996	RSDI	0.187
			$\kappa_1 = 3$	ARL_1	181.374	103.027	60.136	33.074	14.445	4.345	2.271	1.591	RMI	0.044
			$\kappa_2 = 9$	SDRL_1	180.873	102.526	59.634	32.570	13.936	3.812	1.699	0.970	RSDI	0.139
	0.10	EWMA		ARL_1	365.398	358.465	347.245	326.003	270.762	115.519	28.870	5.850	RMI	9.336
				SDRL_1	364.898	357.965	346.745	325.503	270.262	115.018	28.366	5.327	RSDI	10.609
		Modified EWMA		ARL_1	248.749	166.740	107.616	62.974	28.086	7.572	3.294	1.955	RMI	0.628
		with $\kappa = 1$		SDRL_1	248.248	166.239	107.115	62.472	27.581	7.054	2.749	1.366	RSDI	0.692
		Double-Modified EWMA	$\kappa_1 = 1$	ARL_1	237.970	154.960	98.042	56.588	25.059	6.853	3.073	1.879	RMI	0.498
			$\kappa_2 = 1$	SDRL_1	237.469	154.459	97.541	56.086	24.554	6.334	2.524	1.286	RSDI	0.548
			$\kappa_1 = 1$	ARL_1	200.320	118.856	71.024	39.562	17.297	5.020	2.493	1.673	RMI	0.140
			$\kappa_2 = 3$	SDRL_1	199.819	118.355	70.522	39.059	16.789	4.492	1.929	1.062	RSDI	0.154
			$\kappa_1 = 1$	ARL_1	186.285	106.947	62.771	34.622	15.120	4.505	2.325	1.611	RMI	0.033
			$\kappa_2 = 9$	SDRL_1	185.784	106.446	62.269	34.119	14.611	3.974	1.755	0.992	RSDI	0.036
			$\kappa_1 = 3$	ARL_1	181.615	103.217	60.263	33.149	14.478	4.353	2.274	1.592	RMI	0
			$\kappa_2 = 9$	SDRL_1	181.114	102.716	59.761	32.645	13.969	3.821	1.702	0.971	RSDI	0
	0.15	EWMA		ARL_1	365.268	357.699	345.543	322.833	265.545	115.655	34.025	8.881	RMI	9.777
				SDRL_1	364.768	357.199	345.043	322.333	265.045	115.154	33.521	8.366	RSDI	11.291
		Modified EWMA		ARL_1	241.833	159.096	101.352	58.765	26.071	7.078	3.132	1.894	RMI	0.537
		with $\kappa = 1$		SDRL_1	241.332	158.595	100.851	58.263	25.566	6.559	2.584	1.301	RSDI	0.591
		Double-Modified EWMA	$\kappa_1 = 1$	ARL_1	228.045	144.801	90.116	51.446	22.663	6.277	2.886	1.810	RMI	0.387
			$\kappa_2 = 1$	SDRL_1	227.544	144.300	89.614	50.943	22.157	5.755	2.333	1.211	RSDI	0.426
			$\kappa_1 = 1$	ARL_1	197.424	116.357	69.271	38.503	16.826	4.907	2.455	1.659	RMI	0.115
			$\kappa_2 = 3$	SDRL_1	196.923	115.856	68.769	38.000	16.318	4.378	1.889	1.045	RSDI	0.126
			$\kappa_1 = 1$	ARL_1	185.606	106.456	62.452	34.438	15.040	4.487	2.318	1.609	RMI	0.026
			$\kappa_2 = 9$	SDRL_1	185.105	105.955	61.950	33.934	14.532	3.955	1.748	0.990	RSDI	0.029
			$\kappa_1 = 3$	ARL_1	181.891	103.430	60.405	33.232	14.514	4.363	2.278	1.594	RMI	0
			$\kappa_2 = 9$	SDRL_1	181.390	102.929	59.903	32.728	14.005	3.830	1.706	0.973	RSDI	0

Note: UCL values are set as follows: $\lambda = 0.05$: $H_0' = 0.000000007073$ for EWMA, $H_1' = 0.1856261$ for modified EWMA, and $H' = 0.2051786, 0.614691, 1.84316$, and 5.212152 for double-modified EWMA with (κ_1, κ_2) equals $(1,1), (1,3), (1,9), (3,9)$. $\lambda = 0.1$: $H_0' = 0.0002981$ for EWMA, $H_1' = 0.1870737$ for modified EWMA, and $H' = 0.2281136, 0.6765671, 2.022867$, and 5.4263 for double-modified EWMA with (κ_1, κ_2) equals $(1,1), (1,3), (1,9), (3,9)$. $\lambda = 0.2$: $H_0' = 0.005808$ for EWMA, $H_1' = 0.1887875$ for modified EWMA, and $H' = 0.2532332, 0.7409083, 2.206105$, and 5.644353 for double-modified EWMA with (κ_1, κ_2) equals $(1,1), (1,3), (1,9), (3,9)$.

Table A7. Comparative performance of the two-sided EWMA, modified EWMA, and double-modified EWMA control charts with control limits set at $[\mathrm{LCL}, \mathrm{UCL}]$ under the ARFIX$(2, 0.25, 2)$ model using the explicit closed-form solution based on simulated data with parameters $\vartheta = 2$, $\phi_1 = 0.2$, and $\phi_2 = 0.4$ when the determined ARL_0 equals 370.

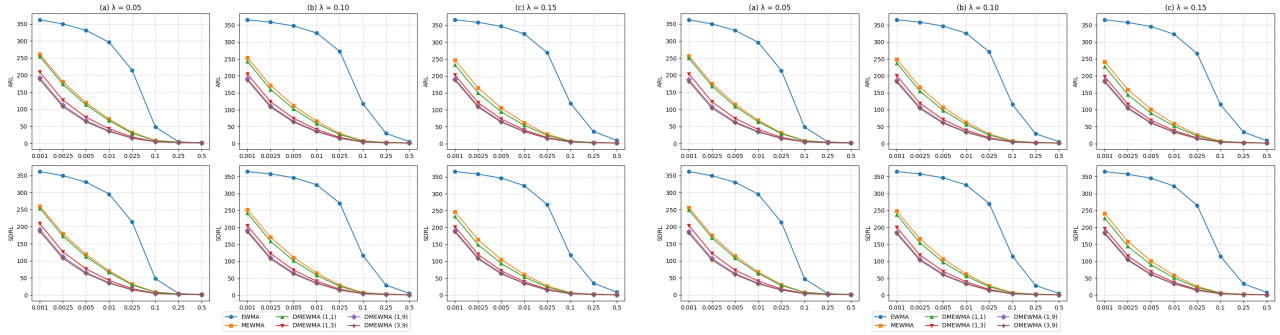
Model	λ	Control Chart	δ	0.001	0.0025	0.005	0.01	0.025	0.1	0.25	0.5	Indices	
ARFIX(2, 0.25, 2)	0.05	EWMA	ARL_1	361.987	349.893	330.704	295.675	212.736	47.292	4.779	1.172	RMI	8.351
			SDRL_1	361.487	349.393	330.204	295.175	212.235	46.789	4.250	0.449	RSDI	9.230
		Modified EWMA	ARL_1	205.366	123.110	73.813	40.977	17.555	4.653	2.113	1.387	RMI	0.656
		with $\kappa = 1$	SDRL_1	204.865	122.609	73.311	40.474	17.048	4.123	1.534	0.732	RSDI	0.776
		Double-Modified EWMA	$\kappa_1 = 1$	198.924	117.331	69.704	38.492	16.472	4.423	2.051	1.369	RMI	0.580
			$\kappa_2 = 1$	198.423	116.830	69.202	37.989	15.964	3.891	1.469	0.710	RSDI	0.688
			$\kappa_1 = 1$	155.033	82.999	46.941	25.295	10.867	3.229	1.721	1.270	RMI	0.158
			$\kappa_2 = 3$	154.532	82.497	46.438	24.790	10.355	2.682	1.114	0.586	RSDI	0.201
			$\kappa_1 = 1$	140.302	72.884	40.678	21.811	9.422	2.918	1.632	1.242	RMI	0.042
			$\kappa_2 = 9$	139.801	72.382	40.175	21.305	8.908	2.366	1.016	0.549	RSDI	0.066
			$\kappa_1 = 3$	135.578	69.776	38.792	20.774	8.995	2.826	1.606	1.234	RMI	0.007
			$\kappa_2 = 9$	135.077	69.274	38.288	20.267	8.480	2.272	0.986	0.537	RSDI	0.024
	0.10	EWMA	ARL_1	364.876	357.113	344.595	321.049	260.829	101.306	22.222	4.155	RMI	13.298
			SDRL_1	364.376	356.613	344.095	320.549	260.329	100.805	21.716	3.621	RSDI	16.091
		Modified EWMA	ARL_1	197.620	116.321	69.022	38.087	16.292	4.378	2.035	1.362	RMI	0.561
		with $\kappa = 1$	SDRL_1	197.119	115.820	68.520	37.583	15.784	3.846	1.451	0.702	RSDI	0.641
		Double-Modified EWMA	$\kappa_1 = 1$	186.654	107.113	62.688	34.334	14.678	4.037	1.943	1.335	RMI	0.444
			$\kappa_2 = 1$	186.153	106.612	62.186	33.830	14.170	3.501	1.354	0.669	RSDI	0.508
			$\kappa_1 = 1$	151.552	80.566	45.420	24.444	10.511	3.151	1.698	1.263	RMI	0.125
			$\kappa_2 = 3$	151.051	80.065	44.917	23.938	9.999	2.604	1.089	0.576	RSDI	0.143
			$\kappa_1 = 1$	139.295	72.211	40.267	21.584	9.328	2.898	1.626	1.240	RMI	0.029
			$\kappa_2 = 9$	138.794	71.709	39.763	21.078	8.814	2.345	1.009	0.546	RSDI	0.033
			$\kappa_1 = 3$	135.369	69.645	38.714	20.731	8.977	2.822	1.604	1.234	RMI	0
			$\kappa_2 = 9$	134.868	69.143	38.210	20.225	8.462	2.268	0.985	0.537	RSDI	0
	0.15	EWMA	ARL_1	362.283	349.934	330.711	296.700	220.663	72.925	17.350	4.201	RMI	10.915
			SDRL_1	361.783	349.434	330.211	296.200	220.162	72.423	16.842	3.667	RSDI	13.136
		Modified EWMA	ARL_1	190.532	110.315	64.866	35.612	15.220	4.144	1.968	1.340	RMI	0.484
		with $\kappa = 1$	SDRL_1	190.031	109.814	64.364	35.109	14.711	3.610	1.380	0.675	RSDI	0.553
		Double-Modified EWMA	$\kappa_1 = 1$	176.984	99.371	57.501	31.308	13.387	3.758	1.864	1.311	RMI	0.349
			$\kappa_2 = 1$	176.483	98.869	56.999	30.804	12.877	3.220	1.270	0.638	RSDI	0.399
			$\kappa_1 = 1$	148.688	78.589	44.191	23.758	10.226	3.089	1.680	1.257	RMI	0.103
			$\kappa_2 = 3$	148.187	78.087	43.688	23.252	9.713	2.540	1.069	0.568	RSDI	0.118
			$\kappa_1 = 1$	138.463	71.655	39.927	21.396	9.250	2.881	1.621	1.239	RMI	0.024
			$\kappa_2 = 9$	137.962	71.153	39.424	20.890	8.736	2.328	1.003	0.544	RSDI	0.027
			$\kappa_1 = 3$	135.315	69.562	38.654	20.695	8.962	2.819	1.603	1.233	RMI	0
			$\kappa_2 = 9$	134.814	69.060	38.150	20.189	8.447	2.264	0.983	0.536	RSDI	0

Note: LCL equal to 0.1, and UCL values are set as follows: $\lambda = 0.05$: $H_0' = 0.100000006325$ for EWMA, $H_1' = 0.12250116$ for modified EWMA, and $H' = 0.1248589, 0.1742379, 0.3223672$, and 0.7286005 for double-modified EWMA with (κ_1, κ_2) equals $(1,1), (1,3), (1,9), (3,9)$. $\lambda = 0.1$: $H_0' = 0.10009218$ for EWMA, $H_1' = 0.12269322$ for modified EWMA, and $H' = 0.12762397, 0.1814858, 0.3431594$, and 0.7518611 for double-modified EWMA with (κ_1, κ_2) equals $(1,1), (1,3), (1,9), (3,9)$. $\lambda = 0.2$: $H_0' = 0.1009515$ for EWMA, $H_1' = 0.12291487$ for modified EWMA, and $H' = 0.13063137, 0.18897273, 0.3642013$, and 0.775378 for double-modified EWMA with (κ_1, κ_2) equals $(1,1), (1,3), (1,9), (3,9)$.

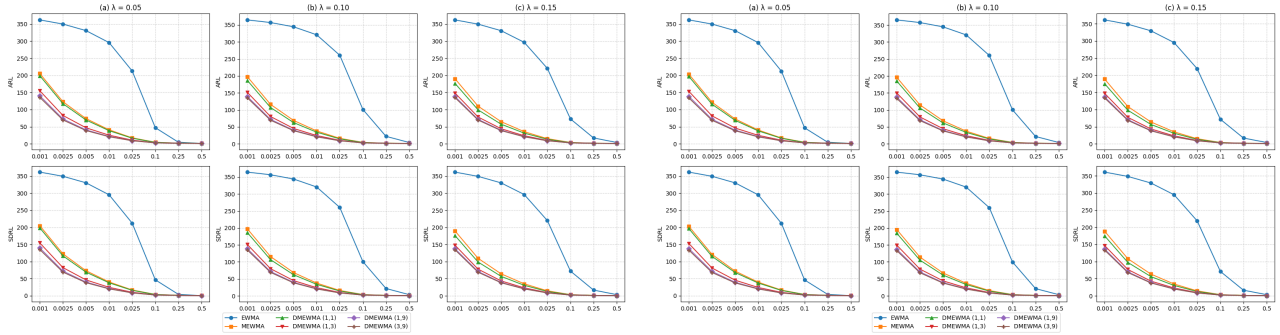
Table A8. Comparative performance of the two-sided EWMA, modified EWMA, and double-modified EWMA control charts with control limits set at $[\mathrm{LCL}, \mathrm{UCL}]$ under the ARFIX$(2, 0.45, 2)$ model using the explicit closed-form solution based on simulated data with parameters $\vartheta = 2$, $\phi_1 = 0.2$, and $\phi_2 = 0.4$ when the determined ARL_0 equals 370.

Model	λ	Control Chart		δ	0.001	0.0025	0.005	0.01	0.025	0.1	0.25	0.5	Indices	
ARFIX(2, 0.45, 2)	0.05	EWMA		ARL_1	362.099	349.951	330.679	295.512	212.322	46.904	4.708	1.167	RMI	8.473
				SDRL_1	361.599	349.451	330.179	295.012	211.821	46.401	4.178	0.441	RSDI	9.379
		Modified EWMA		ARL_1	203.607	121.548	72.695	40.289	17.240	4.569	2.081	1.372	RMI	0.656
		with $\kappa = 1$		SDRL_1	203.106	121.047	72.193	39.786	16.732	4.038	1.499	0.714	RSDI	0.776
		Double-Modified EWMA	$\kappa_1 = 1$	ARL_1	196.935	115.733	68.608	37.834	16.174	4.344	2.020	1.355	RMI	0.579
			$\kappa_2 = 1$	SDRL_1	196.434	115.232	68.106	37.330	15.666	3.811	1.436	0.693	RSDI	0.687
			$\kappa_1 = 1$	ARL_1	153.340	81.788	46.173	24.857	10.675	3.177	1.700	1.260	RMI	0.158
			$\kappa_2 = 3$	SDRL_1	152.839	81.287	45.670	24.352	10.162	2.630	1.091	0.572	RSDI	0.200
			$\kappa_1 = 1$	ARL_1	138.649	71.780	40.000	21.430	9.257	2.874	1.614	1.233	RMI	0.041
			$\kappa_2 = 9$	SDRL_1	138.148	71.279	39.496	20.924	8.743	2.320	0.995	0.536	RSDI	0.065
			$\kappa_1 = 3$	ARL_1	133.953	68.710	38.142	20.411	8.838	2.784	1.588	1.225	RMI	0.006
			$\kappa_2 = 9$	SDRL_1	133.452	68.208	37.639	19.905	8.323	2.228	0.966	0.525	RSDI	0.024
	0.10	EWMA		ARL_1	365.146	357.320	344.702	320.979	260.372	100.450	21.817	4.055	RMI	13.435
				SDRL_1	364.646	356.820	344.202	320.479	259.872	99.949	21.311	3.520	RSDI	16.289
		Modified EWMA		ARL_1	195.865	114.815	67.966	37.446	16.000	4.300	2.004	1.348	RMI	0.561
		with $\kappa = 1$		SDRL_1	195.364	114.314	67.464	36.942	15.492	3.767	1.419	0.685	RSDI	0.642
		Double-Modified EWMA	$\kappa_1 = 1$	ARL_1	184.939	105.691	61.714	33.752	14.416	3.966	1.915	1.323	RMI	0.444
			$\kappa_2 = 1$	SDRL_1	184.438	105.190	61.212	33.248	13.907	3.430	1.324	0.653	RSDI	0.509
			$\kappa_1 = 1$	ARL_1	149.828	79.369	44.669	24.018	10.325	3.101	1.678	1.253	RMI	0.125
			$\kappa_2 = 3$	SDRL_1	149.327	78.867	44.166	23.512	9.813	2.552	1.066	0.563	RSDI	0.143
			$\kappa_1 = 1$	ARL_1	137.597	71.100	39.589	21.205	9.164	2.853	1.607	1.231	RMI	0.029
			$\kappa_2 = 9$	SDRL_1	137.096	70.598	39.086	20.699	8.650	2.300	0.988	0.533	RSDI	0.033
			$\kappa_1 = 3$	ARL_1	133.732	68.575	38.063	20.368	8.820	2.780	1.586	1.225	RMI	0
			$\kappa_2 = 9$	SDRL_1	133.231	68.073	37.559	19.862	8.305	2.224	0.965	0.524	RSDI	0
	0.15	EWMA		ARL_1	361.352	348.894	329.517	295.283	218.982	71.780	16.937	4.086	RMI	10.968
				SDRL_1	360.852	348.394	329.017	294.783	218.481	71.278	16.430	3.551	RSDI	13.221
		Modified EWMA		ARL_1	188.839	108.879	63.871	35.013	14.949	4.072	1.940	1.327	RMI	0.485
		with $\kappa = 1$		SDRL_1	188.338	108.378	63.369	34.510	14.441	3.537	1.350	0.659	RSDI	0.554
		Double-Modified EWMA	$\kappa_1 = 1$	ARL_1	175.268	98.013	56.594	30.774	13.149	3.695	1.839	1.299	RMI	0.349
			$\kappa_2 = 1$	SDRL_1	174.767	97.511	56.092	30.270	12.639	3.155	1.242	0.623	RSDI	0.399
			$\kappa_1 = 1$	ARL_1	147.084	77.442	43.467	23.346	10.046	3.040	1.660	1.247	RMI	0.103
			$\kappa_2 = 3$	SDRL_1	146.583	76.940	42.964	22.840	9.532	2.490	1.046	0.555	RSDI	0.118
			$\kappa_1 = 1$	ARL_1	136.787	70.553	39.254	21.020	9.088	2.837	1.602	1.229	RMI	0.024
			$\kappa_2 = 9$	SDRL_1	136.286	70.051	38.751	20.514	8.573	2.282	0.983	0.531	RSDI	0.027
			$\kappa_1 = 3$	ARL_1	133.619	68.475	37.997	20.330	8.804	2.776	1.585	1.224	RMI	0
			$\kappa_2 = 9$	SDRL_1	133.118	67.973	37.494	19.824	8.289	2.221	0.963	0.524	RSDI	0

Note: LCL equal to 0.1, and UCL values are set as follows: $\lambda = 0.05$: $H_0' = 0.100000005742$ for EWMA, $H_1' = 0.12041765$ for modified EWMA, and $H' = 0.12255682, 0.167364, 0.3017774$, and 0.6703962 for double-modified EWMA with (κ_1, κ_2) equals $(1,1), (1,3), (1,9), (3,9)$. $\lambda = 0.1$: $H_0' = 0.10008371$ for EWMA, $H_1' = 0.12059101$ for modified EWMA, and $H' = 0.12506504, 0.17393694, 0.3206325$, and 0.6914722 for double-modified EWMA with (κ_1, κ_2) equals $(1,1), (1,3), (1,9), (3,9)$. $\lambda = 0.2$: $H_0' = 0.10086273$ for EWMA, $H_1' = 0.12079132$ for modified EWMA, and $H' = 0.1277926, 0.1807268, 0.3397131$, and 0.712777 for double-modified EWMA with (κ_1, κ_2) equals $(1,1), (1,3), (1,9), (3,9)$.

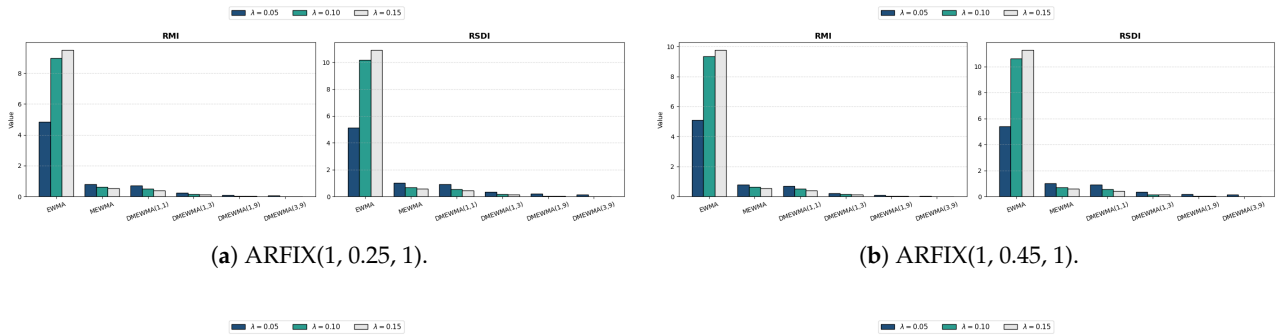


(**a**) ARFIX(1, 0.25, 1). (**b**) ARFIX(1, 0.45, 1).

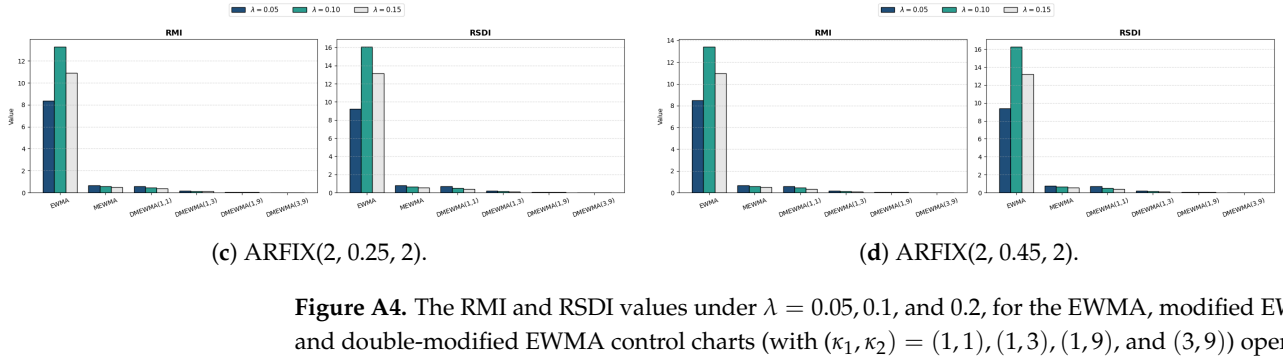


(**c**) ARFIX(2, 0.25, 2). (**d**) ARFIX(2, 0.45, 2).

Figure A3. The ARL_1 and $SDRL_1$ values vary with the magnitude of the shift (δ), from small-to-moderate levels, under $\lambda = 0.05, 0.1$, and 0.2, for the EWMA, modified EWMA, and double-modified EWMA control charts (with $(\kappa_1, \kappa_2) = (1,1), (1,3), (1,9)$, and $(3,9)$) operating under the ARFIX(p, d, r) model: (**a**) ARFIX$(1, 0.25, 1)$, (**b**) ARFIX$(1, 0.45, 1)$, (**c**) ARFIX$(2, 0.25, 2)$, and (**d**) ARFIX$(2, 0.45, 2)$.



(**a**) ARFIX(1, 0.25, 1). (**b**) ARFIX(1, 0.45, 1).



(**c**) ARFIX(2, 0.25, 2). (**d**) ARFIX(2, 0.45, 2).

Figure A4. The RMI and RSDI values under $\lambda = 0.05, 0.1$, and 0.2, for the EWMA, modified EWMA, and double-modified EWMA control charts (with $(\kappa_1, \kappa_2) = (1,1), (1,3), (1,9)$, and $(3,9)$) operating under the ARFIX(p, d, r) model: (**a**) ARFIX$(1, 0.25, 1)$, (**b**) ARFIX$(1, 0.45, 1)$, (**c**) ARFIX$(2, 0.25, 2)$, and (**d**) ARFIX$(2, 0.45, 2)$.

Table A9. Comparative performance of the EWMA-type control charts with control limits set at $[0, \text{UCL}]$ under the ARX$(1,2)$ model using the explicit closed-form solution based on monthly dataset of WTI crude oil prices (unit: USD) with two exogenous variables (US Dollar Index and Volatility Index) with parameters $\vartheta = 0, \phi_1 = 0.9649, b_1 = 0.0596$, and $b_2 = -0.1990$ when the determined ARL_0 equals 370 following exponential white noise with $\alpha_0 = 4.6764$.

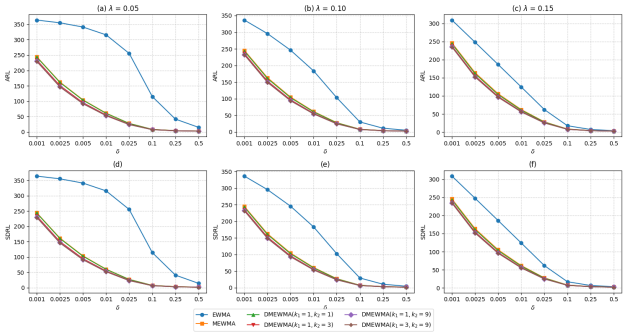
Model	λ	Control Chart		δ	0.001	0.0025	0.005	0.01	0.025	0.1	0.25	0.5	Indices	
ARX(1, 2)	0.05	EWMA		ARL_1	364.159	355.343	341.395	316.010	255.504	114.946	41.610	14.789	RMI	6.367
				SDRL_1	363.659	354.843	340.895	315.510	255.004	114.445	41.107	14.280	RSDI	7.018
		Modified EWMA		ARL_1	244.577	162.340	104.265	61.066	27.677	8.117	3.926	2.499	RMI	0.122
		with $\kappa = 1$		SDRL_1	244.076	161.839	103.764	60.564	27.172	7.600	3.389	1.935	RSDI	0.130
		Double-Modified EWMA	$\kappa_1 = 1$	ARL_1	243.275	160.847	103.015	60.230	27.270	8.010	3.887	2.483	RMI	0.110
			$\kappa_2 = 1$	SDRL_1	242.774	160.346	102.514	59.727	26.765	7.493	3.350	1.918	RSDI	0.118
			$\kappa_1 = 1$	ARL_1	233.919	150.867	95.041	54.938	24.734	7.348	3.645	2.379	RMI	0.034
			$\kappa_2 = 3$	SDRL_1	233.418	150.366	94.540	54.436	24.229	6.829	3.105	1.812	RSDI	0.036
			$\kappa_1 = 1$	ARL_1	230.476	147.390	92.340	53.184	23.905	7.132	3.566	2.345	RMI	0.008
			$\kappa_2 = 9$	SDRL_1	229.975	146.889	91.839	52.681	23.400	6.613	3.025	1.776	RSDI	0.009
			$\kappa_1 = 3$	ARL_1	229.248	146.218	91.451	52.614	23.638	7.063	3.540	2.334	RMI	0
			$\kappa_2 = 9$	SDRL_1	228.747	145.717	90.950	52.112	23.133	6.543	2.999	1.764	RSDI	0
	0.10	EWMA		ARL_1	336.607	295.864	245.970	183.461	102.918	30.015	11.208	5.154	RMI	1.887
				SDRL_1	336.107	295.364	245.469	182.960	102.417	29.511	10.696	4.627	RSDI	2.027
		Modified EWMA		ARL_1	245.403	163.183	104.939	61.517	27.898	8.180	3.953	2.514	RMI	0.105
		with $\kappa = 1$		SDRL_1	244.902	162.682	104.438	61.015	27.393	7.664	3.417	1.951	RSDI	0.112
		Double-Modified EWMA	$\kappa_1 = 1$	ARL_1	243.116	160.705	102.923	60.165	27.245	8.010	3.892	2.488	RMI	0.086
			$\kappa_2 = 1$	SDRL_1	242.615	160.204	102.422	59.663	26.740	7.493	3.355	1.924	RSDI	0.092
			$\kappa_1 = 1$	ARL_1	235.760	152.841	96.615	55.979	25.237	7.488	3.703	2.409	RMI	0.027
			$\kappa_2 = 3$	SDRL_1	235.259	152.340	96.114	55.477	24.732	6.970	3.164	1.842	RSDI	0.029
			$\kappa_1 = 1$	ARL_1	232.930	149.970	94.372	54.516	24.544	7.308	3.637	2.381	RMI	0.007
			$\kappa_2 = 9$	SDRL_1	232.429	149.469	93.871	54.014	24.039	6.789	3.097	1.813	RSDI	0.007
			$\kappa_1 = 3$	ARL_1	232.048	149.062	93.662	54.053	24.325	7.251	3.617	2.372	RMI	0
			$\kappa_2 = 9$	SDRL_1	231.547	148.561	93.160	53.551	23.819	6.732	3.076	1.804	RSDI	0
	0.15	EWMA		ARL_1	309.521	248.270	186.614	124.551	62.098	17.382	7.059	3.684	RMI	0.922
				SDRL_1	309.021	247.769	186.113	124.050	61.596	16.874	6.540	3.144	RSDI	0.983
		Modified EWMA		ARL_1	246.308	164.204	105.785	62.094	28.184	8.262	3.988	2.532	RMI	0.088
		with $\kappa = 1$		SDRL_1	245.807	163.703	105.284	61.592	27.679	7.746	3.452	1.969	RSDI	0.094
		Double-Modified EWMA	$\kappa_1 = 1$	ARL_1	243.862	161.368	103.424	60.491	27.404	8.059	3.916	2.502	RMI	0.067
			$\kappa_2 = 1$	SDRL_1	243.361	160.867	102.923	59.989	26.900	7.543	3.379	1.939	RSDI	0.071
			$\kappa_1 = 1$	ARL_1	237.870	155.094	98.416	57.173	25.816	7.648	3.769	2.442	RMI	0.022
			$\kappa_2 = 3$	SDRL_1	237.369	154.593	97.915	56.671	25.311	7.131	3.230	1.877	RSDI	0.023
			$\kappa_1 = 1$	ARL_1	235.694	152.797	96.590	55.970	25.242	7.500	3.715	2.420	RMI	0.005
			$\kappa_2 = 9$	SDRL_1	235.193	152.296	96.088	55.468	24.737	6.982	3.176	1.854	RSDI	0.006
			$\kappa_1 = 3$	ARL_1	234.959	152.052	96.007	55.589	25.061	7.453	3.699	2.413	RMI	0
			$\kappa_2 = 9$	SDRL_1	234.458	151.551	95.506	55.087	24.556	6.935	3.159	1.847	RSDI	0

Note: LCL equal to 0, and UCL values are set as follows: $\lambda = 0.05$: $H_0 = 0.143671$ for EWMA, $H_1 = 4.154942$ for modified EWMA, and $H = 4.57495, 13.37528, 39.776$, and 112.1781 for double-modified EWMA with (κ_1, κ_2) equals $(1,1), (1,3), (1,9), (3,9)$. $\lambda = 0.1$: $H_0 = 0.323378$ for EWMA, $H_1 = 4.406182$ for modified EWMA, and $H = 5.305707, 15.1198, 44.5632$, and 118.99 for double-modified EWMA with (κ_1, κ_2) equals $(1,1), (1,3), (1,9), (3,9)$. $\lambda = 0.2$: $H_0 = 0.497475$ for EWMA, $H_1 = 4.668741$ for modified EWMA, and $H = 6.11182, 16.9897, 49.6262$, and 126.1972 for double-modified EWMA with (κ_1, κ_2) equals $(1,1), (1,3), (1,9), (3,9)$.

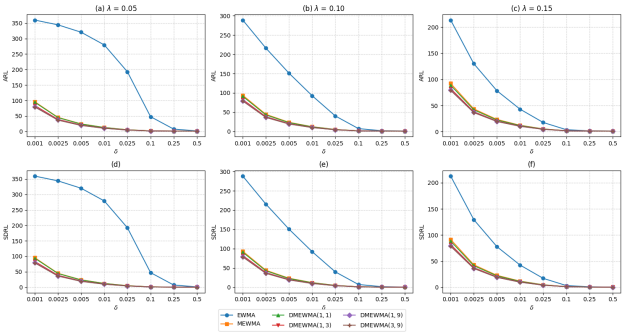
Table A10. Comparative performance of the EWMA-type control charts with control limits set at $[0, \text{UCL}]$ under the ARFIX$(1, 0.14, 2)$ model using the explicit closed-form solution based on monthly dataset of Brent crude oil prices (unit: USD) with two exogenous variables (WTI crude oil prices and US treasury 10Y yield) with parameters $\vartheta = 0, \phi_1 = 0.5156, b_1 = 0.3416$, and $b_2 = -1.3053$ when determined ARL_0 equals 370 following exponential white noise with $\alpha_0 = 3.3817$.

Model	λ	Control Chart	δ	0.001	0.0025	0.005	0.01	0.025	0.1	0.25	0.5	Indices	
ARFIX(1, 0.14, 2)	0.05	EWMA	ARL_1	359.720	344.238	320.483	279.486	192.752	47.792	7.663	1.705	RMI	16.154
			SDRL_1	359.220	343.738	319.983	278.986	192.251	47.289	7.146	1.096	RSDI	21.014
		Modified EWMA	ARL_1	95.811	45.558	24.464	12.861	5.533	1.828	1.181	1.039	RMI	0.166
		with $\kappa = 1$	SDRL_1	95.310	45.055	23.959	12.351	5.009	1.230	0.462	0.200	RSDI	0.204
		Double-Modified EWMA	$\kappa_1 = 1$	94.076	44.614	23.940	12.590	5.429	1.810	1.177	1.038	RMI	0.148
			$\kappa_2 = 1$	93.575	44.111	23.434	12.079	4.904	1.211	0.457	0.199	RSDI	0.183
			$\kappa_1 = 1$	83.557	38.913	20.782	10.957	4.803	1.702	1.157	1.034	RMI	0.044
			$\kappa_2 = 3$	83.056	38.410	20.276	10.445	4.274	1.093	0.426	0.188	RSDI	0.055
			$\kappa_1 = 1$	80.043	37.076	19.779	10.442	4.606	1.668	1.150	1.033	RMI	0.011
			$\kappa_2 = 9$	79.541	36.573	19.273	9.929	4.076	1.056	0.415	0.185	RSDI	0.013
			$\kappa_1 = 3$	78.928	36.494	19.461	10.279	4.544	1.657	1.148	1.033	RMI	0
			$\kappa_2 = 9$	78.427	35.991	18.955	9.766	4.013	1.044	0.412	0.184	RSDI	0
	0.10	EWMA	ARL_1	288.627	215.931	151.003	92.723	40.381	7.621	2.107	1.167	RMI	4.354
			SDRL_1	288.127	215.430	150.502	92.221	39.878	7.103	1.527	0.441	RSDI	5.241
		Modified EWMA	ARL_1	93.939	44.522	23.885	12.560	5.417	1.808	1.177	1.038	RMI	0.147
		with $\kappa = 1$	SDRL_1	93.438	44.019	23.380	12.050	4.892	1.208	0.456	0.198	RSDI	0.181
		Double-Modified EWMA	$\kappa_1 = 1$	91.161	43.014	23.048	12.127	5.251	1.779	1.171	1.037	RMI	0.120
			$\kappa_2 = 1$	90.660	42.511	22.543	11.616	4.725	1.177	0.448	0.195	RSDI	0.147
			$\kappa_1 = 1$	82.759	38.491	20.551	10.838	4.757	1.694	1.155	1.034	RMI	0.037
			$\kappa_2 = 3$	82.258	37.987	20.044	10.325	4.228	1.085	0.423	0.187	RSDI	0.046
			$\kappa_1 = 1$	79.803	36.949	19.709	10.406	4.593	1.666	1.149	1.033	RMI	0.009
			$\kappa_2 = 9$	79.301	36.445	19.203	9.893	4.062	1.053	0.414	0.185	RSDI	0.011
			$\kappa_1 = 3$	78.880	36.466	19.446	10.271	4.541	1.657	1.148	1.033	RMI	0
			$\kappa_2 = 9$	78.378	35.963	18.939	9.758	4.010	1.043	0.412	0.184	RSDI	0
	0.15	EWMA	ARL_1	213.319	129.941	78.207	43.000	17.578	3.807	1.517	1.089	RMI	1.879
			SDRL_1	212.818	129.440	77.705	42.497	17.071	3.269	0.885	0.311	RSDI	2.253
		Modified EWMA	ARL_1	92.206	43.584	23.365	12.291	5.313	1.789	1.173	1.037	RMI	0.130
		with $\kappa = 1$	SDRL_1	91.704	43.081	22.860	11.780	4.787	1.188	0.450	0.196	RSDI	0.160
		Double-Modified EWMA	$\kappa_1 = 1$	88.851	41.762	22.355	11.768	5.113	1.755	1.167	1.036	RMI	0.097
			$\kappa_2 = 1$	88.349	41.259	21.849	11.257	4.586	1.151	0.441	0.193	RSDI	0.119
			$\kappa_1 = 1$	82.084	38.139	20.359	10.739	4.720	1.688	1.154	1.034	RMI	0.031
			$\kappa_2 = 3$	81.583	37.636	19.852	10.227	4.190	1.077	0.421	0.187	RSDI	0.038
			$\kappa_1 = 1$	79.592	36.840	19.650	10.376	4.581	1.664	1.149	1.033	RMI	0.007
			$\kappa_2 = 9$	79.091	36.337	19.144	9.863	4.050	1.051	0.414	0.184	RSDI	0.009
			$\kappa_1 = 3$	78.854	36.445	19.433	10.263	4.538	1.656	1.148	1.033	RMI	0
			$\kappa_2 = 9$	78.353	35.941	18.926	9.750	4.007	1.043	0.412	0.184	RSDI	0

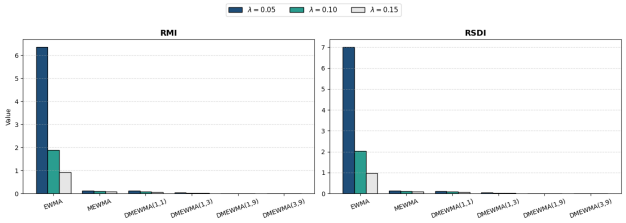
Note: LCL equal to 0, and UCL values are set as follows: $\lambda = 0.05$: $H_0' = 0.00000763$ for EWMA, $H_1' = 0.00036931$ for modified EWMA, and $H' = 0.000406793, 0.00119221, 0.00354843$, and 0.010010212 for double-modified EWMA with (κ_1, κ_2) equals $(1,1), (1,3), (1,9), (3,9)$. $\lambda = 0.1$: $H_0' = 0.00002564$ for EWMA, $H_1' = 0.00038201$ for modified EWMA, and $H' = 0.00046053, 0.00131729, 0.0038877$, and 0.0103852 for double-modified EWMA with (κ_1, κ_2) equals $(1,1), (1,3), (1,9), (3,9)$. $\lambda = 0.2$: $H_0' = 0.00003938$ for EWMA, $H_1' = 0.000394763$ for modified EWMA, and $H' = 0.000517865, 0.00144595, 0.00423054$, and 0.0107638 for double-modified EWMA with (κ_1, κ_2) equals $(1,1), (1,3), (1,9), (3,9)$.



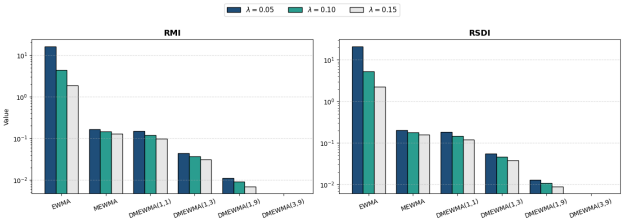
(**a**) ARL and SDRL values based on ARX(1, 2).



(**b**) ARL and SDRL values based on ARFIX(1, 0.14, 2).

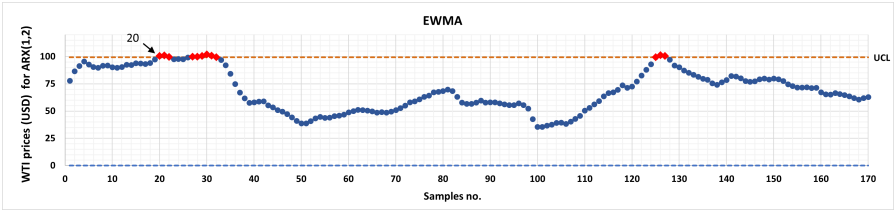


(**c**) RMI and RSDI values based on ARX(1, 2).

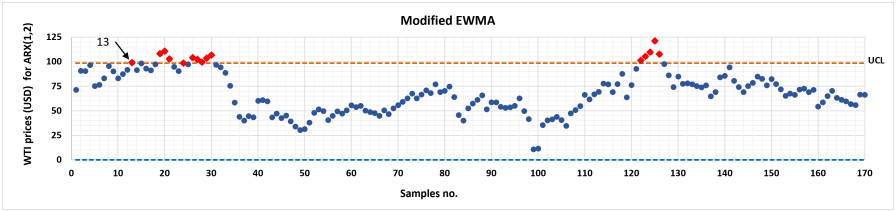


(**d**) RMI and RSDI values based on ARFIX(1, 0.14, 2).

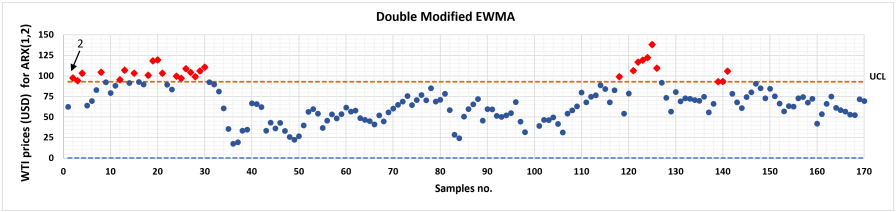
Figure A5. Comparative performance measures based on two datasets, namely WTI and Brent crude oil prices, are presented for the fitted ARX(1, 2) and ARFIX(1, 0.14, 2) models, respectively: (**a**) ARL and SDRL for the ARX(1, 2) model, (**b**) ARL and SDRL for the ARFIX(1, 0.14, 2) model, (**c**) RMI and RSDI for the ARX(1, 2) model, and (**d**) RMI and RSDI for the ARFIX(1, 0.14, 2) model.



(**a**) EWMA.

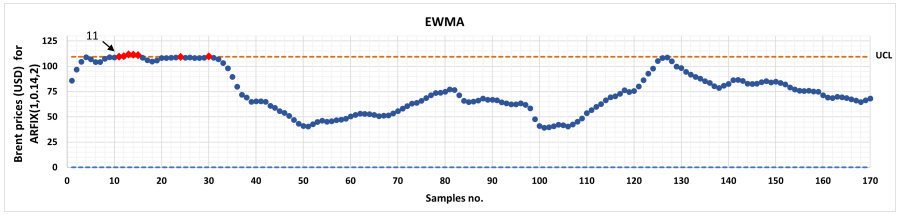


(**b**) Modified EWMA.

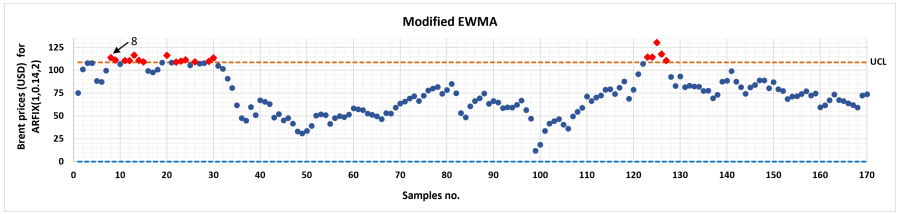


(**c**) Double-Modified EWMA.

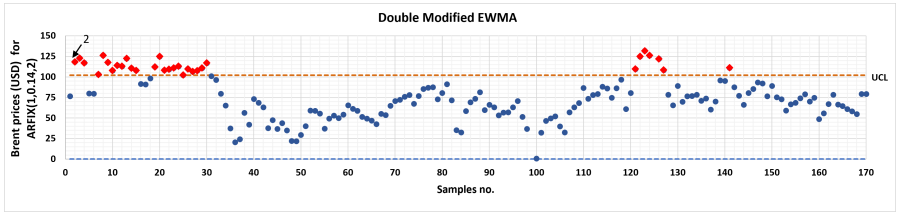
Figure A6. The detection performance of control charts, including (**a**) EWMA, (**b**) modified EWMA, and (**c**) double-modified EWMA, all defined with $\lambda = 0.3$, is assessed under the ARX(1, 2) model using monthly WTI crude oil prices over the period from January 2012 to February 2026, with two exogenous variables, namely the US Dollar Index and the Volatility Index.



(**a**) EWMA.



(**b**) Modified EWMA.



(**c**) Double-Modified EWMA.

Figure A7. The detection performance of control charts, including (**a**) EWMA, (**b**) modified EWMA, and (**c**) double-modified EWMA, all defined with $\lambda = 0.3$, is assessed under the ARFIX(1, 0.14, 2) model using monthly Brent crude oil prices over the period from January 2012 to February 2026, with two exogenous variables, namely the WTI crude oil prices and the US treasury 10Y yield.

Appendix B

Appendix B.1. Existence and Uniqueness of ARL Under an AR Model with Exogenous Variables

Banach's fixed-point theorem [37] is used to justify the existence and uniqueness of the ARL solution obtained from the integral equation. Based on Equation (8), the integral equation can be rewritten in operator form. Let $\gamma[L, H]$ be the space of continuous functions on $[L, H]$, and define the operator $T : \gamma[L, H]$ to $\gamma[L, H]$ by Equation (A1) as follows below.

$$T(\Pi(v)) = 1 + \frac{1}{\eta}\int_{L}^{H} \Pi(\varsigma) f\left(\frac{\varsigma - \rho v + Qu + Q'\omega}{\eta} - \vartheta - \sum_{j=1}^{r} b_j x_{1-j}\right) d\varsigma \qquad \text{(A1)}$$

If T is a contraction mapping, then the fixed-point equation $T(\Pi(v)) = \Pi(v)$ has a unique solution. Hence, the ARL integral equation is well-defined. The proof for the ARX(p, r) model under the DMEWMA chart is given as follows.

Let $\Pi_1, \Pi_2 \in \gamma([L, H])$ and define the supremum norm by

Consider

$$\|T(\Pi_1) - T(\Pi_2)\|_{\infty}.$$

Proof. The difference between their images under the operator T is bounded as follows:

$$
\begin{aligned}
&= \sup_{v\in[L,H]} |T(\Pi_1(v)) - T(\Pi_2(v))| \\
&= \sup_{v\in[L,H]} \left| \frac{\exp\left(\frac{\rho v - Qu - Q'\omega}{\eta\alpha} + \frac{\vartheta + \sum_{j=1}^{r} b_j x_{1-j}}{\alpha}\right)}{\eta\alpha} \int_L^H (\Pi_1(\varsigma) - \Pi_2(\varsigma)) M_0(\varsigma)\, d\varsigma \right| \\
&\leq \sup_{v\in[L,H]} \frac{|\exp\left(\frac{\rho v - Qu - Q'\omega}{\eta\alpha} + \frac{\vartheta + \sum_{j=1}^{r} b_j x_{1-j}}{\alpha}\right)|}{\eta\alpha} \int_L^H |\Pi_1(\varsigma) - \Pi_2(\varsigma)| M_0(\varsigma)\, d\varsigma \\
&\leq \|\Pi_1 - \Pi_2\|_\infty \sup_{v\in[L,H]} |\exp\left(\frac{\rho v - Qu - Q'\omega}{\eta\alpha} + \frac{\vartheta + \sum_{j=1}^{r} b_j x_{1-j}}{\alpha}\right)| |M_0(L) - M_0(H)| \\
&= \gamma \|\Pi_1 - \Pi_2\|_\infty,
\end{aligned}
$$

where

$$
\gamma = \sup_{v\in[L,H]} |\exp\left(\frac{\rho v - Qu - Q'\omega}{\eta\alpha} + \frac{\vartheta + \sum_{j=1}^{r} b_j x_{1-j}}{\alpha}\right)| |M_0(L) - M_0(H)|, \quad 0 \leq \gamma < 1.
$$

As a result, T is a mapping that contracts. The unique solution of the ARL integral problem is given by Banach's fixed-point theorem. □

Appendix B.2. Existence and Uniqueness of ARL Under an ARFI Model with Exogenous Variables

The proof follows the same contraction argument as in the previous case. In this case, the term F is subtracted in the argument of the density function. Thus, only the modified operator and its corresponding contraction bound are presented.

Let $\Gamma[L', H']$ denote the space of continuous functions on $[L', H']$ equipped with the supremum norm

$$
\|\Omega\|_\infty = \sup_{v\in[L',H']} |\Omega(v)|.
$$

Define the operator $T : \Gamma[L', H'] \to \Gamma[L', H']$ by

$$
T(\Omega(v)) = 1 + \frac{1}{\eta} \int_{L'}^{H'} \Omega(\varsigma) f\left(\frac{\varsigma - \rho v + Qu + Q'\omega}{\eta} - \vartheta - \sum_{j=1}^{r} b_j x_{1-j} - F\right) d\varsigma. \tag{A2}
$$

Proof. For any $\Omega_1, \Omega_2 \in \Gamma[L', H']$, we obtain $\|T(\Omega_1) - T(\Omega_2)\|_\infty$ as below.

$$
\begin{aligned}
&= \sup_{v\in[L',H']} |T(\Omega_1(v)) - T(\Omega_2(v))| \\
&= \sup_{v\in[L',H']} \left| \frac{\exp\left(\frac{\rho v - Qu - Q'\omega}{\eta\alpha} + \frac{\vartheta + \sum_{j=1}^{r} b_j x_{1-j} + F}{\alpha}\right)}{\eta\alpha} \int_{L'}^{H'} (\Omega_1(\varsigma) - \Omega_2(\varsigma)) M_0(\varsigma)\, d\varsigma \right| \\
&\leq \sup_{v\in[L',H']} \frac{|\exp\left(\frac{\rho v - Qu - Q'\omega}{\eta\alpha} + \frac{\vartheta + \sum_{j=1}^{r} b_j x_{1-j} + F}{\alpha}\right)|}{\eta\alpha} \int_{L'}^{H'} |\Omega_1(\varsigma) - \Omega_2(\varsigma)| M_0(\varsigma)\, d\varsigma
\end{aligned}
$$

$$\leq \|\Omega_1 - \Omega_2\|_\infty \sup_{v\in[L',H']} |\exp\left(\frac{\rho v - Qu - Q'\omega}{\eta\alpha} + \frac{\vartheta + \sum_{j=1}^{r} b_j x_{1-j} + F}{\alpha}\right)||M_0(L') - M_0(H')|$$

$$= \Gamma\|\Omega_1 - \Omega_2\|_\infty,$$

where

$$\Gamma = \sup_{v\in[L',H']} |\exp\left(\frac{\rho v - Qu - Q'\omega}{\eta\alpha} + \frac{\vartheta + \sum_{j=1}^{r} b_j x_{1-j} + F}{\alpha}\right)||M_0(L') - M_0(H')|, 0 \leq \Gamma < 1.$$

That is why T is a contracting mapping. In the case of the ARL integral issue, Banach's fixed-point theorem provides the one and only solution. □

As shown in Appendixes B.1 and B.2, Banach's fixed-point theorem ensures the existence and uniqueness of the ARL solutions associated with the ARX(p, r) and ARFIX(p, d, r) models under the proposed control chart.

References

1. Suman, G.; Prajapati, D. Control chart applications in healthcare: A literature review. *Int. J. Metrol. Qual. Eng.* **2018**, *9*, 5. [CrossRef] [PubMed]
2. Kovarik, M.; Šarga, L.; Klímek, P. Usage of control charts for time series analysis in financial management. *J. Bus. Econ. Manag.* **2015**, *16*, 138–158. [CrossRef]
3. Morrison, L. The use of control charts to interpret environmental monitoring data. *Nat. Areas J.* **2008**, *28*, 66–73. [CrossRef]
4. Alshahrani, F.; Almanjahie, I.M.; Khan, M.; Anwar, S.M.; Rasheed, Z.; Cheema, A.N. On designing of Bayesian Shewhart-type control charts for Maxwell distributed processes with application of boring machine. *Mathematics* **2023**, *11*, 1126. [CrossRef]
5. Anwar, S.M.; Aslam, M.; Ahmad, S.; Riaz, M. A modified-mxEWMA location chart for the improved process monitoring using auxiliary information and its application in wood industry. *Qual. Technol. Quant. Manag.* **2020**, *17*, 561–579. [CrossRef]
6. Scheitrum, D.P.; Carter, C.A.; Revoredo-Giha, C. WTI and Brent futures pricing structure. *Nergy Econ.* **2018**, *72*, 462–469. [CrossRef]
7. Mastroeni, L.; Mazzoccoli, A.; Quaresima, G.; Vellucci, P. Decoupling and recoupling in the crude oil price benchmarks: An investigation of similarity patterns. *Energy Econ.* **2021**, *94*, 105036. [CrossRef]
8. Shewhart, W.A. The application of statistics as an aid in maintaining quality of a manufactured product. *J. Am. Stat. Assoc.* **1925**, *20*, 546–548. [CrossRef]
9. Page, E.S. Continuous inspection schemes. *Biometrika* **1954**, *41*, 100–115. [CrossRef]
10. Roberts, S.W. Control chart tests based on qeometric moving averages. *Technometrics* **1959**, *1*, 239–250. [CrossRef]
11. Patel, A.K.; Divecha, J. Modified exponentially weighted moving average (EWMA) control chart for an analytical process data. *J. Chem. Eng. Mater. Sci.* **2011**, *2*, 12–20.
12. Khan, N.; Aslam, M.; Jun, C. Design of a control chart using a modified EWMA statistic. *Qual. Reliab. Eng. Int.* **2016**, *33*, 1095–1104. [CrossRef]
13. Shamma, S.E.; Shamma, A.K. Development and evaluation of control charts using double exponentially weighted moving averages. *Int. J. Qual. Reliab. Manag.* **1992**, *9*, 18–25. [CrossRef]
14. Naveed, M.; Azam, M.; Khan, N.; Aslam, M. Design of a control chart using extended EWMA statistic *Technologies* **2018**, *6*, 108. [CrossRef]
15. Javed, H.; Ismail, M.; Saeed, N. New extended exponentially weighted moving average control chart for monitoring process mean *Technometrics* **2024**, *10*, e34424. [CrossRef] [PubMed]
16. Alevizakos, V.; Chatterjee, K.; Koukouvinos, C. Modified EWMA and DEWMA control charts for process monitoring. *Commun. Stat. Theory Methods* **2022**, *51*, 7390–7412. [CrossRef]
17. Pinto, D.D.D.; Monteiro, J.G.M.S.; Nakao, E.H. An approach to portfolio selection using an ARX predictor for securities' risk and return. *Expert Syst. Appl.* **2011**, *38*, 15009–15013. [CrossRef]
18. Kristiansen, T. Forecasting Nord Pool day-ahead prices with an autoregressive model with exogenous variables. *Energy Policy* **2012**, *49*, 328–332. [CrossRef]
19. Charfeddine, L.; Zaidan, E.; Alban, A.Q.; Bennasr, H.; Abulibdeh, A. Modeling and forecasting electricity consumption amid the COVID-19 pandemic: Machine learning vs. nonlinear econometric time series models. *Sustain. Cities Soc.* **2023**, *98*, 104860. [CrossRef]

20. Champ, C.W.; Rigdon, S.E. A comparison of the Markov chain and the integral equation approaches for evaluating the run length distribution of quality control charts. *Commun. Stat. Simul. Comput.* **1991**, *20*, 191–204. [CrossRef]
21. Fu, M.C.; Hu, J. Efficient design and sensitivity analysis of control charts using Monte Carlo simulation. *Manag. Sci.* **1999**, *45*, 395–413. [CrossRef]
22. Phanyaem, S. Explicit formulas and numerical integral equation of ARL for SARX(P,r)$_L$ model based on CUSUM chart. *Math. Stat.* **2022**, *10*, 88–99. [CrossRef]
23. Peerajit, W.; Areepong, Y. Alternative to Detecting Changes in the Mean of an Autoregressive Fractionally Integrated Process with Exponential White Noise Running on the Modified EWMA Control Chart. *Processes* **2023**, *11*, 503. [CrossRef]
24. Polyeam, D.; Phanyaem, S. Application of EWMA Control Chart for Analyzing Changes in SAR(P)$_L$ Model with Quadratic Trend. *Math. Stat.* **2025**, *13*, 163–174. [CrossRef]
25. Jirawattanapalin, Y.; Phanyeam, S. Development of EWMA Control Chart for Detecting Changes in AR(p) with Quadratic Trend Model. *Malays. J. Fundam. Appl. Sci.* **2026**, *22*, 73–89. [CrossRef]
26. Karoon, K.; Areepong, Y. Capability of New Modified EWMA Control Chart for Integrated and Fractionally Integrated Time-Series: Application to US Stock Prices. *Symmetry* **2026**, *18*, 5. [CrossRef]
27. Paichit, P. An Integral Equation Procedure for Average Run Length of Control Chart of ARX(p) Processes. *Far East J. Math. Sci.* **2016**, *99*, 359–373. [CrossRef]
28. Okhrin, Y.; Schmid, W. Stochastic inequalities for the run length of the EWMA chart for long-memory processes. *REVSTAT J.* **2019**, *17*, 67–90. [CrossRef]
29. Silpakob, K.; Areepong, Y.; Sukparungsee, S.; Sunthornwat, R. Explicit Analytical Solutions for the Average Run Length of Modified EWMA Control Chart for ARX(p,r) Processes. *Songklanakarin J. Sci. Technol.* **2021**, *43*, 1414–1427. [CrossRef]
30. Bualuang, D.; Peerajit, W. Performance of the CUSUM Control Chart Using Approximation to ARL for Long-Memory Fractionally Integrated Autoregressive Process with Exogenous Variable. *Appl. Sci. Eng. Prog.* **2022**, *16*, 5917. [CrossRef]
31. Peerajit, W. Optimizing the EWMA Control Chart to Detect Changes in the Mean of a Long-Memory Seasonal Fractionally Integrated Moving Average and an Exogenous Variable Process with Exponential White Noise and its Application to Electrical Output Data. *WSEAS Trans. Syst. Control* **2025**, *20*, 25–41. [CrossRef]
32. Mcleod, I.; Hipel, K.W. Simulation Procedures for Box-Jenkins Models. *Water Resour. Res.* **1978**, *14*, 969–975. [CrossRef]
33. Almousa, M. Adomian decomposition method with modified Bernstein polynomials for solving nonlinear Fredholm and Volterra integral equations. *Math. Stat.* **2020**, *8*, 278–285. [CrossRef]
34. Kilian, L. Not all oil price shocks are alike: Disentangling demand and supply shocks in the crude oil market. *Am. Econ. Rev.* **2009**, *99*, 1053–1069. [CrossRef]
35. Aloui, R.; Hammoudeh, S.; Nguyen, D.K. A time-varying copula approach to oil and stock market dependence: The case of transition economies. *Energy Econ.* **2013**, *39*, 208–221. [CrossRef]
36. Abuzayed, B.; Al-Fayoumi, N. Risk spillover from crude oil prices to GCC stock market returns: New evidence during the COVID-19 outbreak. *North Am. J. Econ. Financ.* **2021**, *58*, 101476. [CrossRef]
37. Granas, A.; Dugundji, J. *Fixed Point Theory*; Springer: New York, NY, USA, 2003. [CrossRef]

Disclaimer/Publisher's Note: The statements, opinions and data contained in all publications are solely those of the individual author(s) and contributor(s) and not of MDPI and/or the editor(s). MDPI and/or the editor(s) disclaim responsibility for any injury to people or property resulting from any ideas, methods, instructions or products referred to in the content.